Satellite Estimates of Air-Sea Interactions and Feedbacks

Dudley Chelton
Oregon State University

with help from

Larry O'Neill
Peter Gaube
Ricardo Matano
Vincent Combes
Xiaoqing Chu

Ocean Mesoscale Eddy Interactions with the Atmosphere Workshop
Portland, Oregon, February 17, 2018

Overview

1. Air-sea interactions in mesoscale SST frontal regions.
2. Mesoscale eddy influence on SST and wind speed.
3. Eddy-induced SST influence on Ekman pumping.
4. Eddy-induced surface current influence on Ekman pumping.

Overview

1. Air-sea interactions in mesoscale SST frontal regions.
2. Mesoscale eddy influence on SST and wind speed.
3. Eddy-induced SST influence on Ekman pumping.
4. Eddy-induced surface current influence on Ekman pumping.

5. Some modeling results to assess the relative importances of SST versus surface current influences of eddies on Ekman pumping.

Air-Sea Interaction in SST Frontal Regions

Tropical Instability Wave Effects on SST and Wind Stress
(from Chelton et al., 2001 J. Climate)

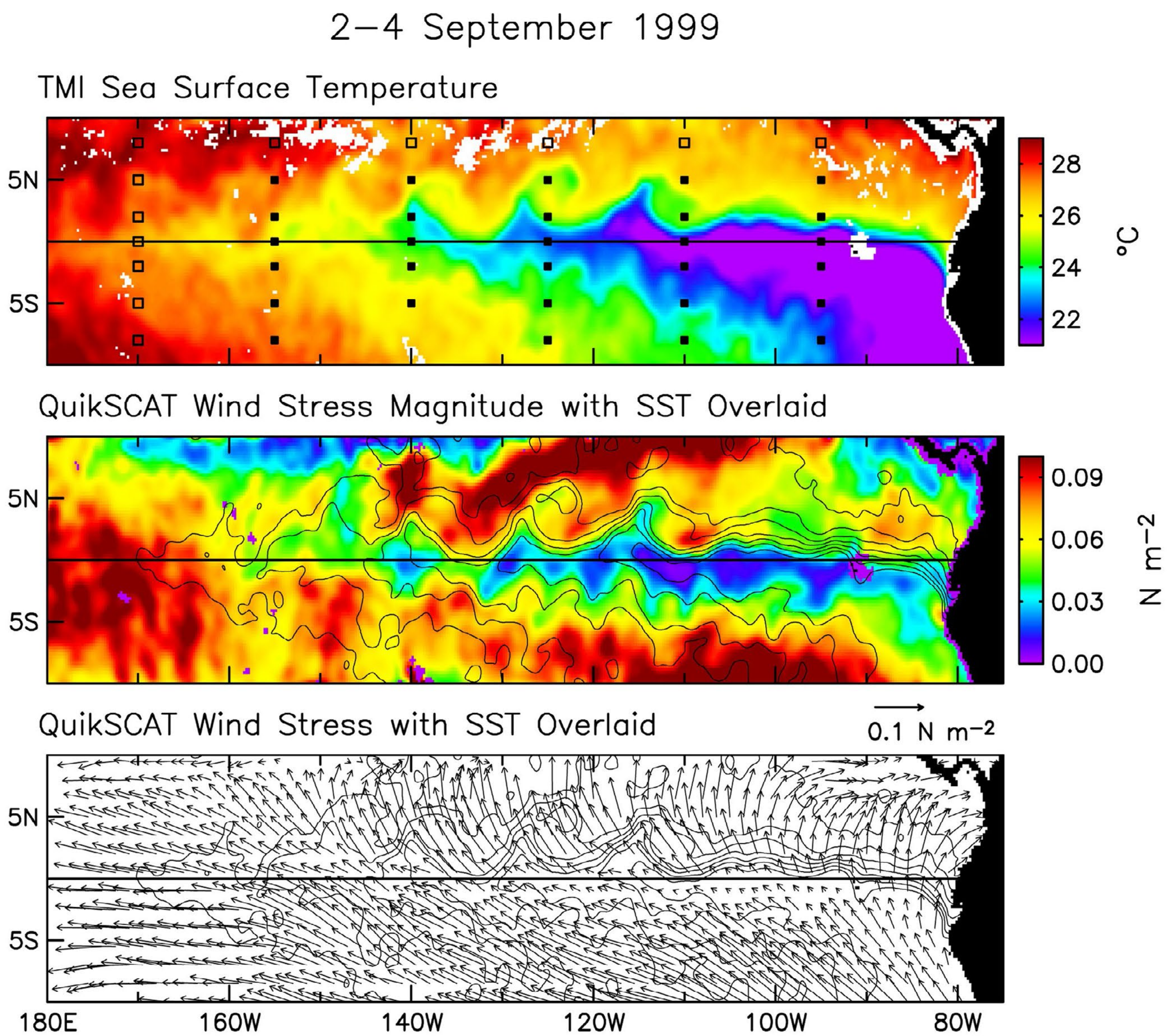

The Coupling Between SST and Wind Stress in 4 Frontal Regions

(Gulf Stream, Kuroshio Extension, Agulhas Return Current and Brazil-Malvinas Current)

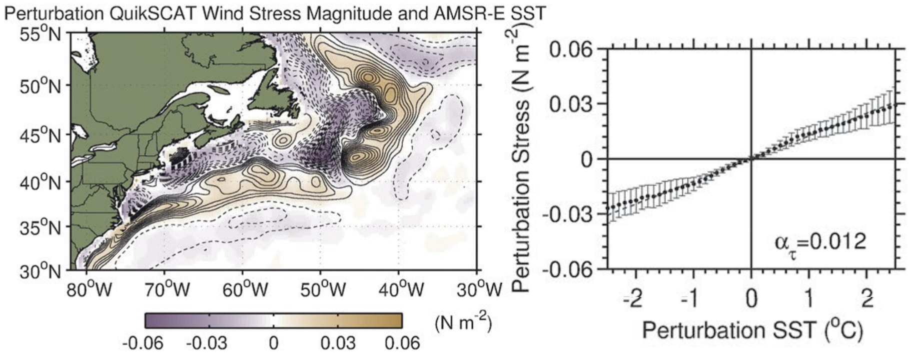

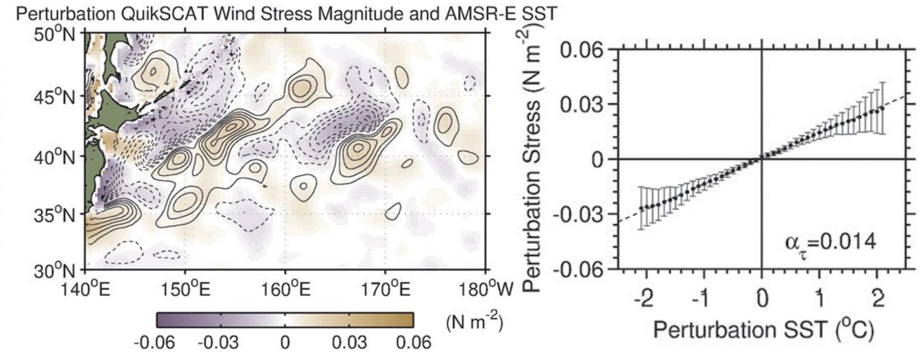

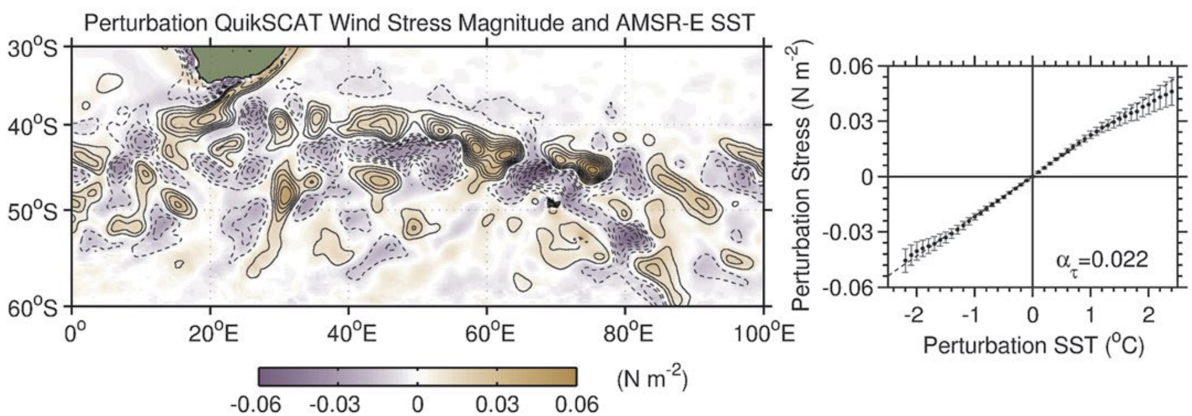

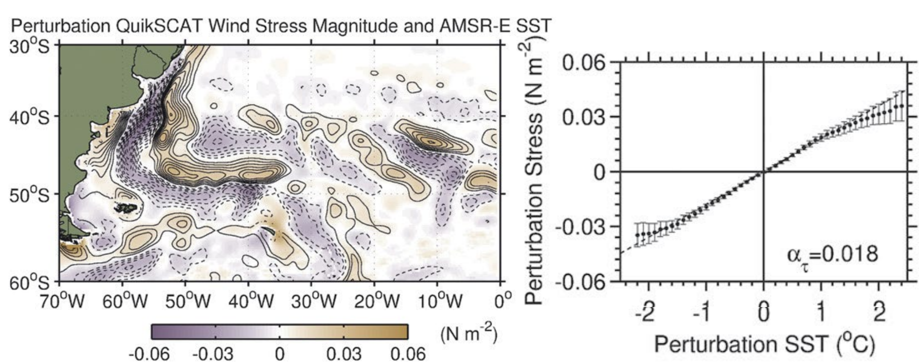

June 2002 - May 2009
Averages

From O'Neill et al. (2012, J. Clim.)

The Coupling Between SST and Wind Speed in 4 Frontal Regions

(Gulf Stream, Kuroshio Extension, Agulhas Return Current and Brazil-Malvinas Current)

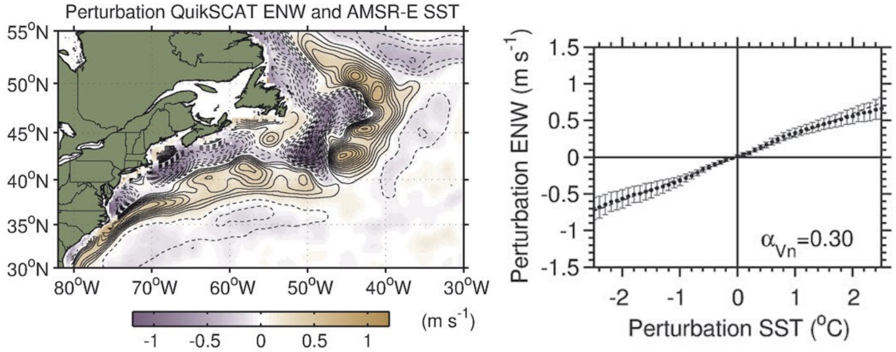

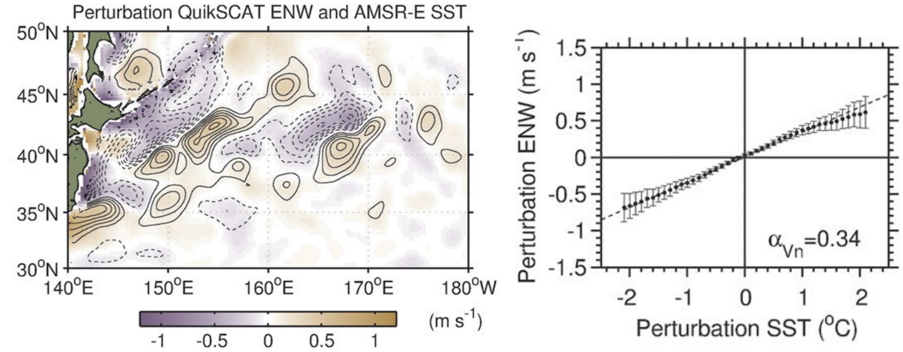

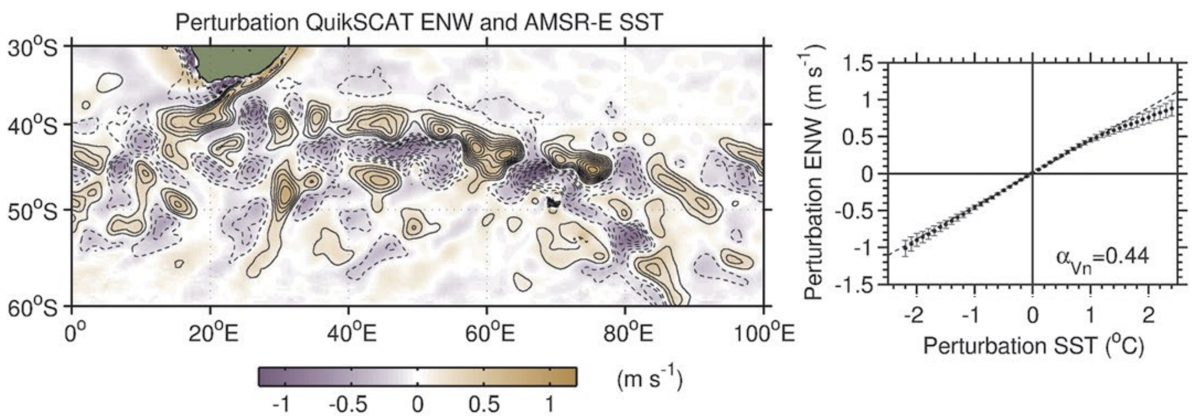

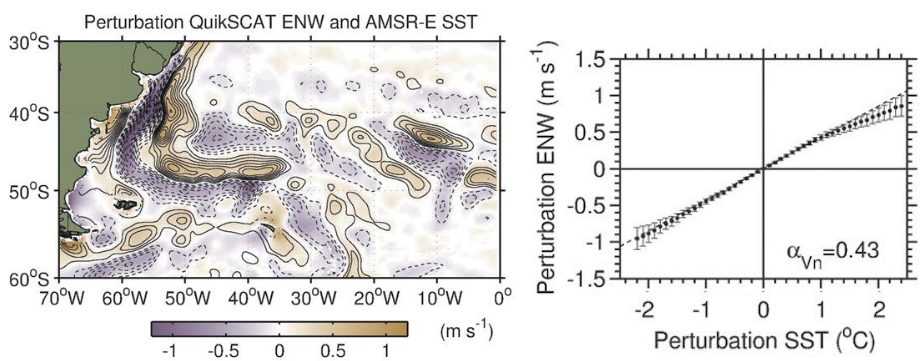

June 2002 - May 2009
Averages

From O'Neill et al. (2012, J. Clim.)

Animation of Coupled Small-Scale Winds and SST in the Gulf Stream Region

July 2002 - September 2009

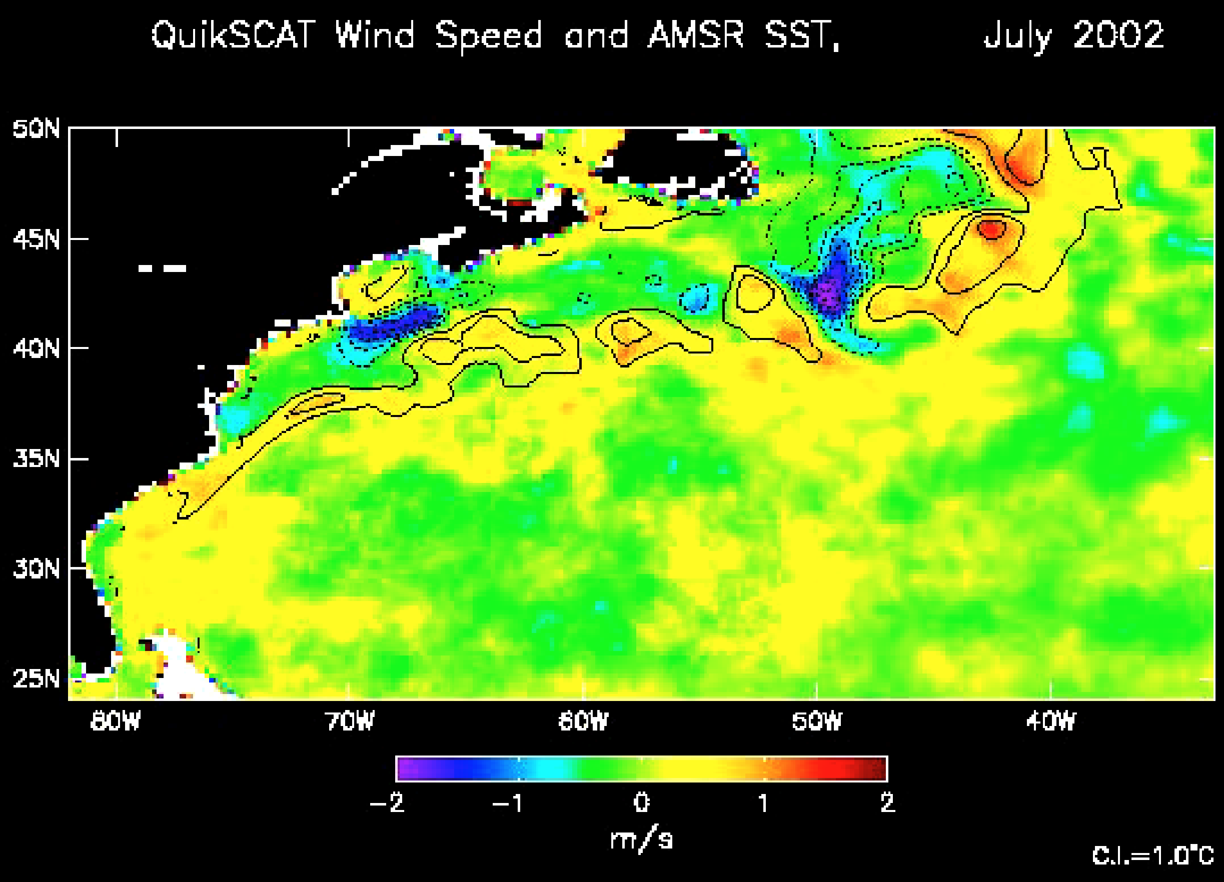

Why the SST influence on surface winds matters.....

SST Effects on the Curl and Divergence of Surface Wind and Stress

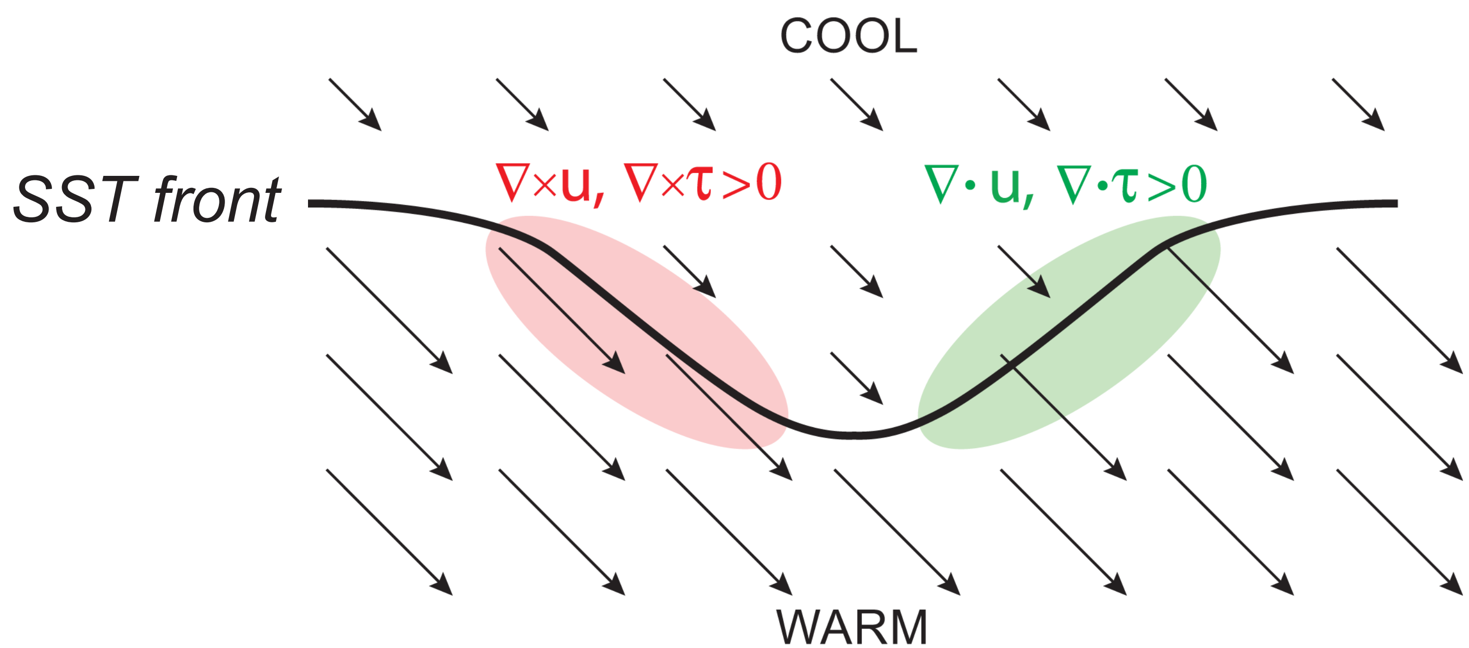

Wind vorticity and curl of the wind stress associated with crosswind SST gradients

Wind divergence and wind stress divergence associated with downwind SST gradients

Coupling Between Wind Stress Divergence and Downwind SST Gradient

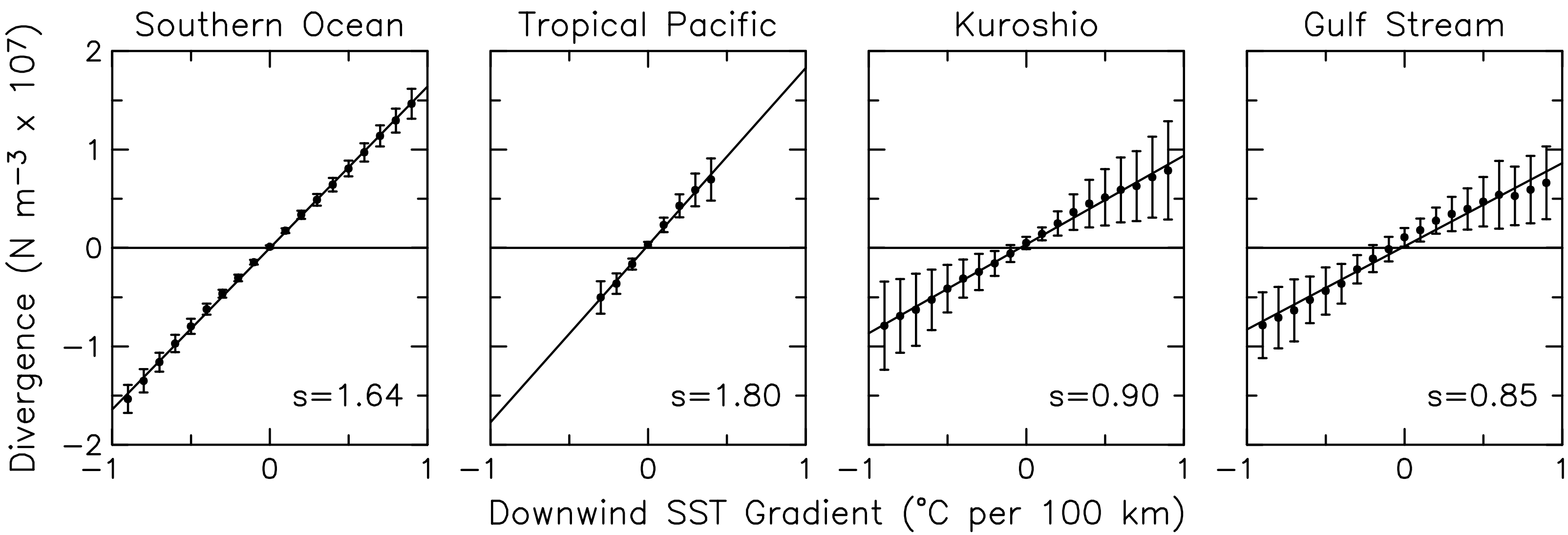

Coupling Between Wind Stress Curl and Crosswind SST Gradient

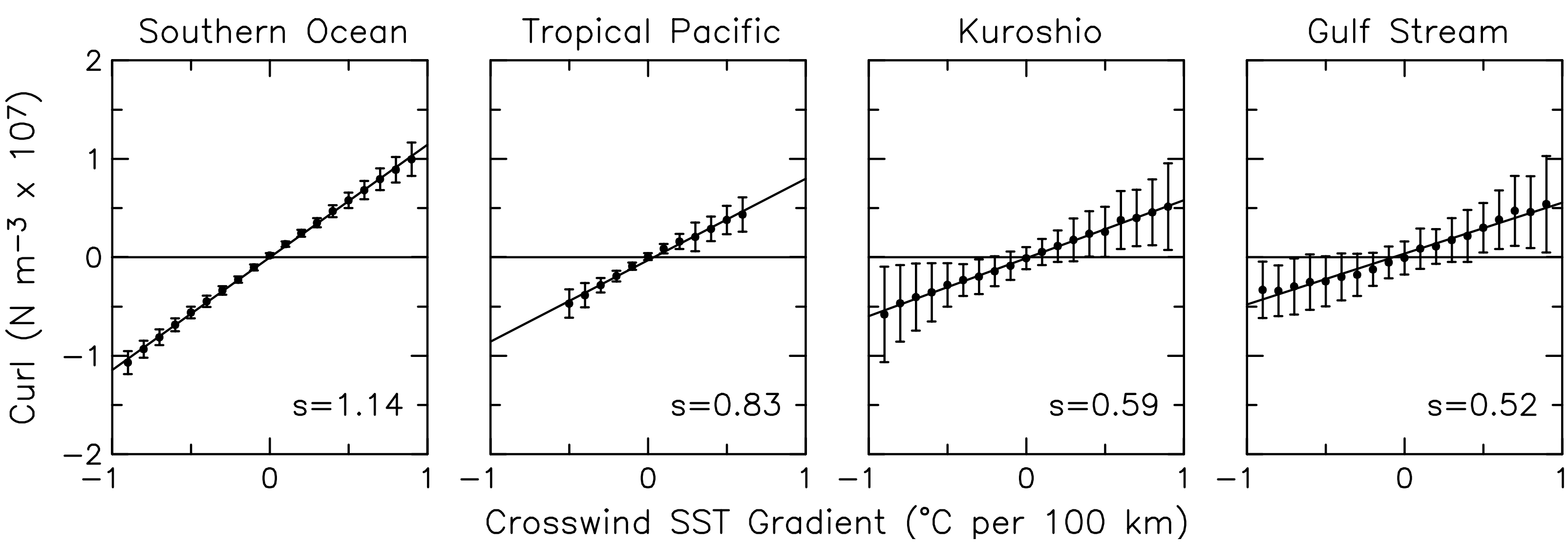

Note that divergence response is consistently stronger than curl response.

A regional example: The California Current System

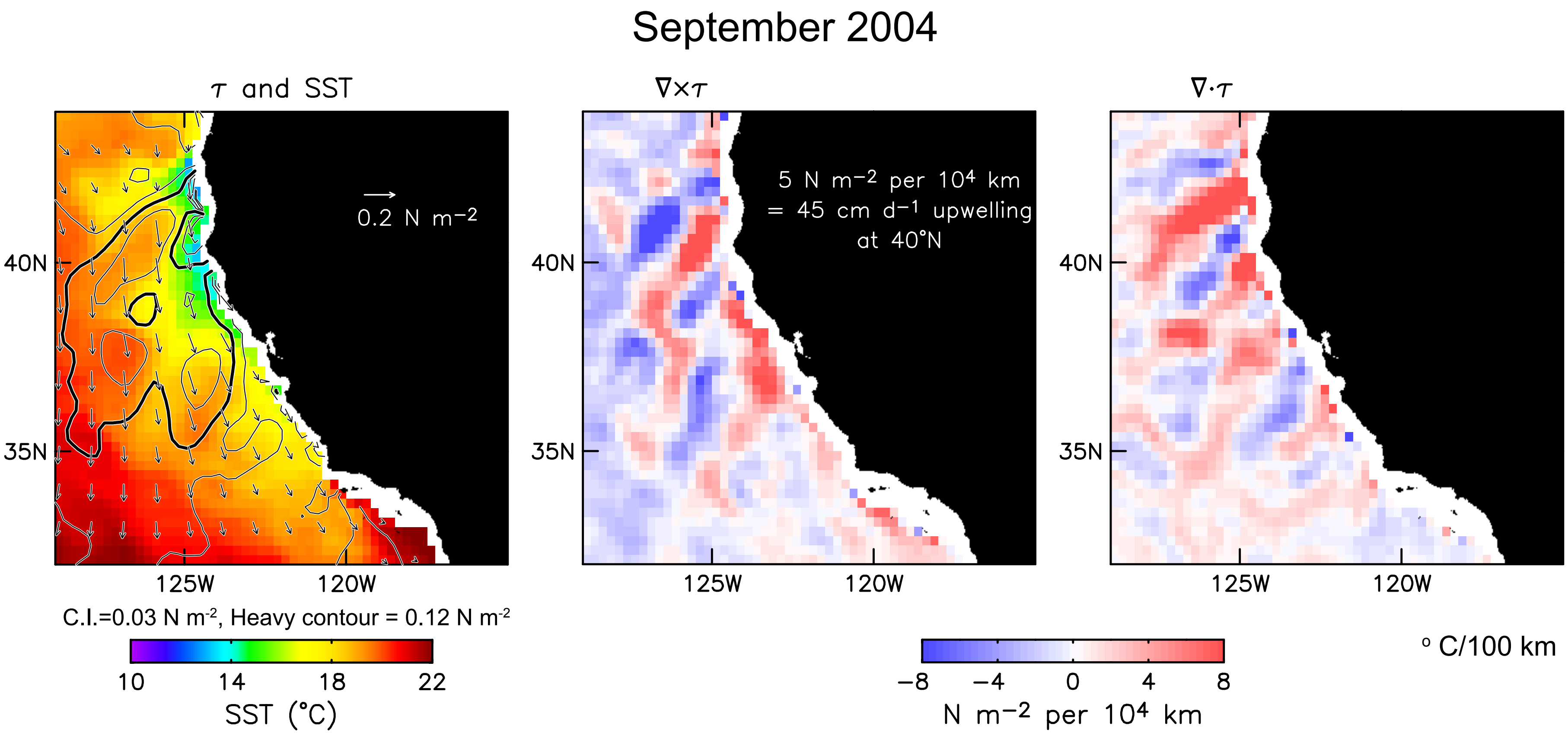

A regional example: The California Current System

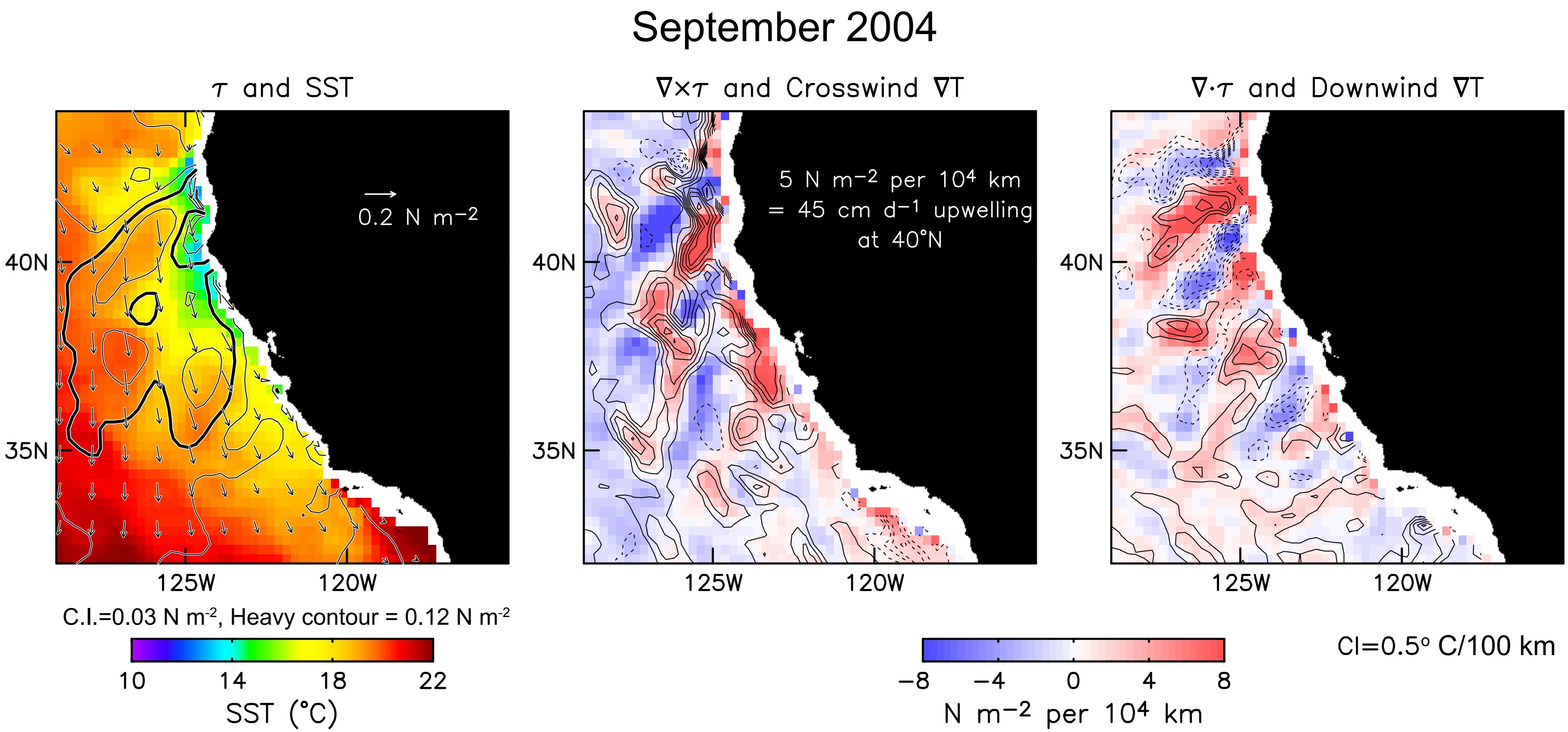

Mesoscale eddy influence on SST and wind speed

Merged TOPEX and ERS-1 Spatially High-Pass Filtered SSH with contours of eddies with lifetimes ≥ 4 weeks

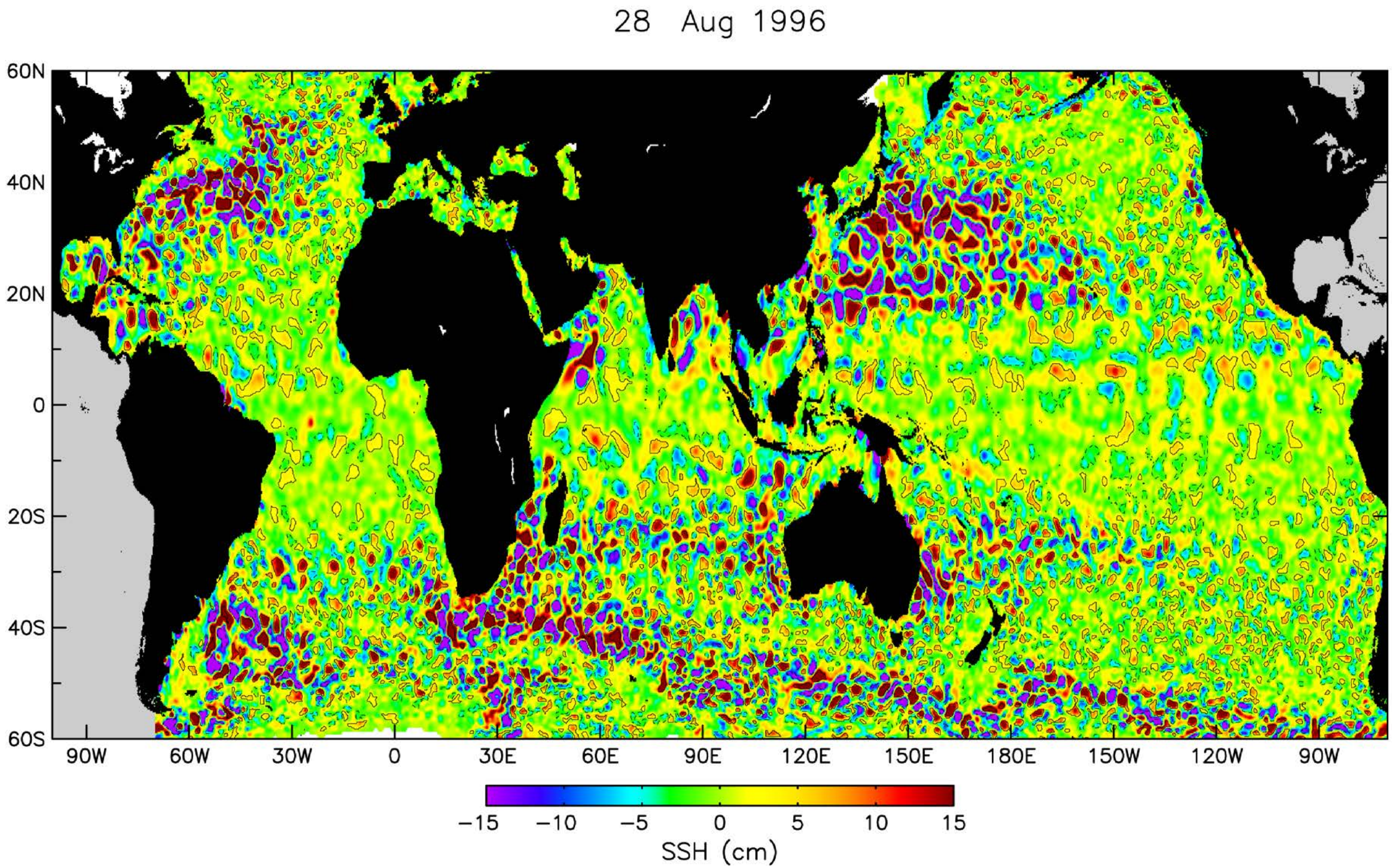

There are 2495 eddies in this map
(http://cioss.coas.oregonstate.edu/eddies/)

Trajectories of the ~22,000 Mesoscale Eddies with Lifemes ≥16 Weeks During the 7.5 Years of Overlap of the Four Satellite Datasets

1 June 2002 - 30 November 2009

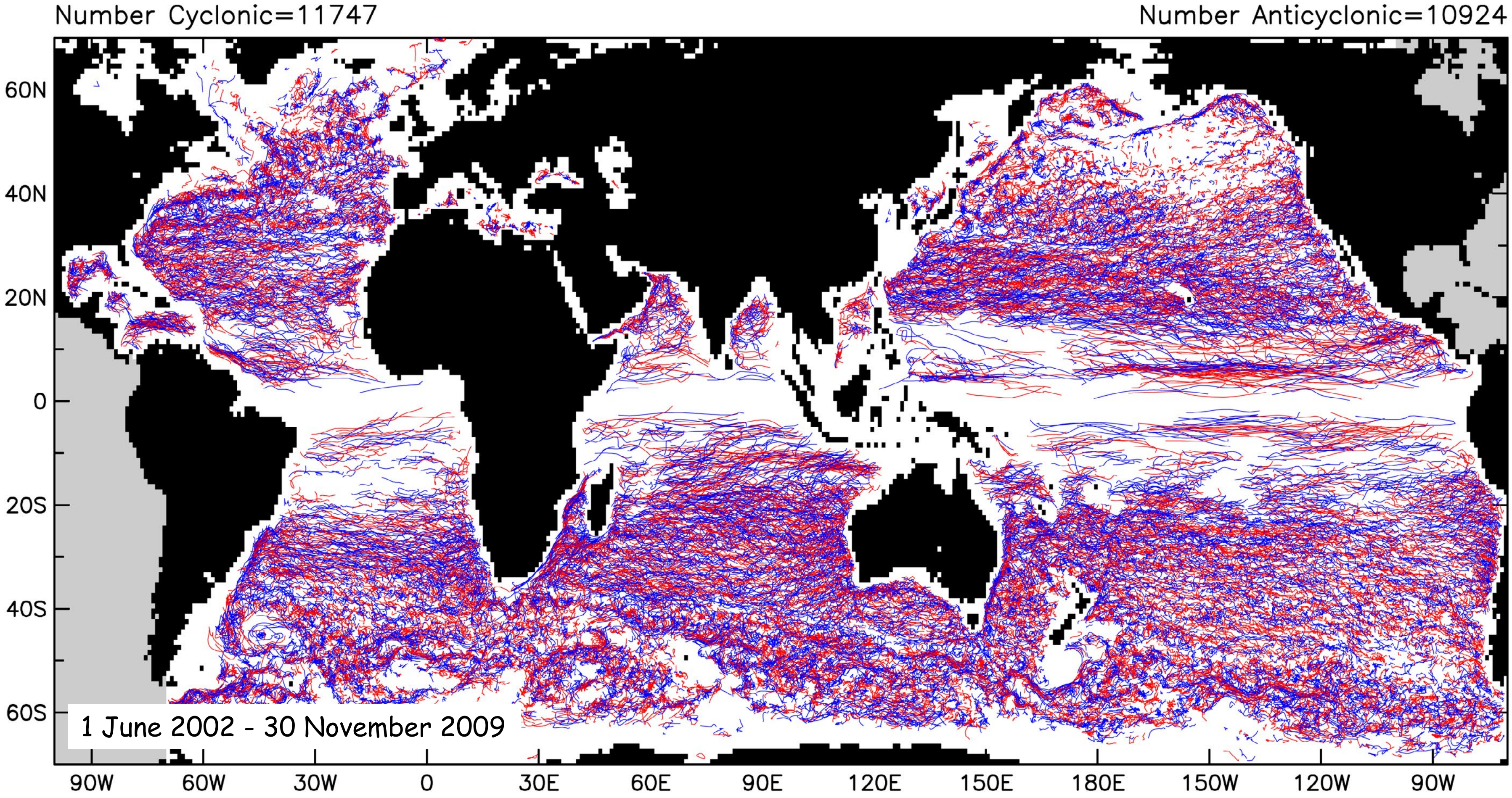

http://cioss.coas.oregonstate.edu/eddies/

Trajectories of the ~22,000 Mesoscale Eddies with Lifemes ≥16 Weeks During the 7.5 Years of Overlap of the Four Satellite Datasets

1 June 2002 - 30 November 2009

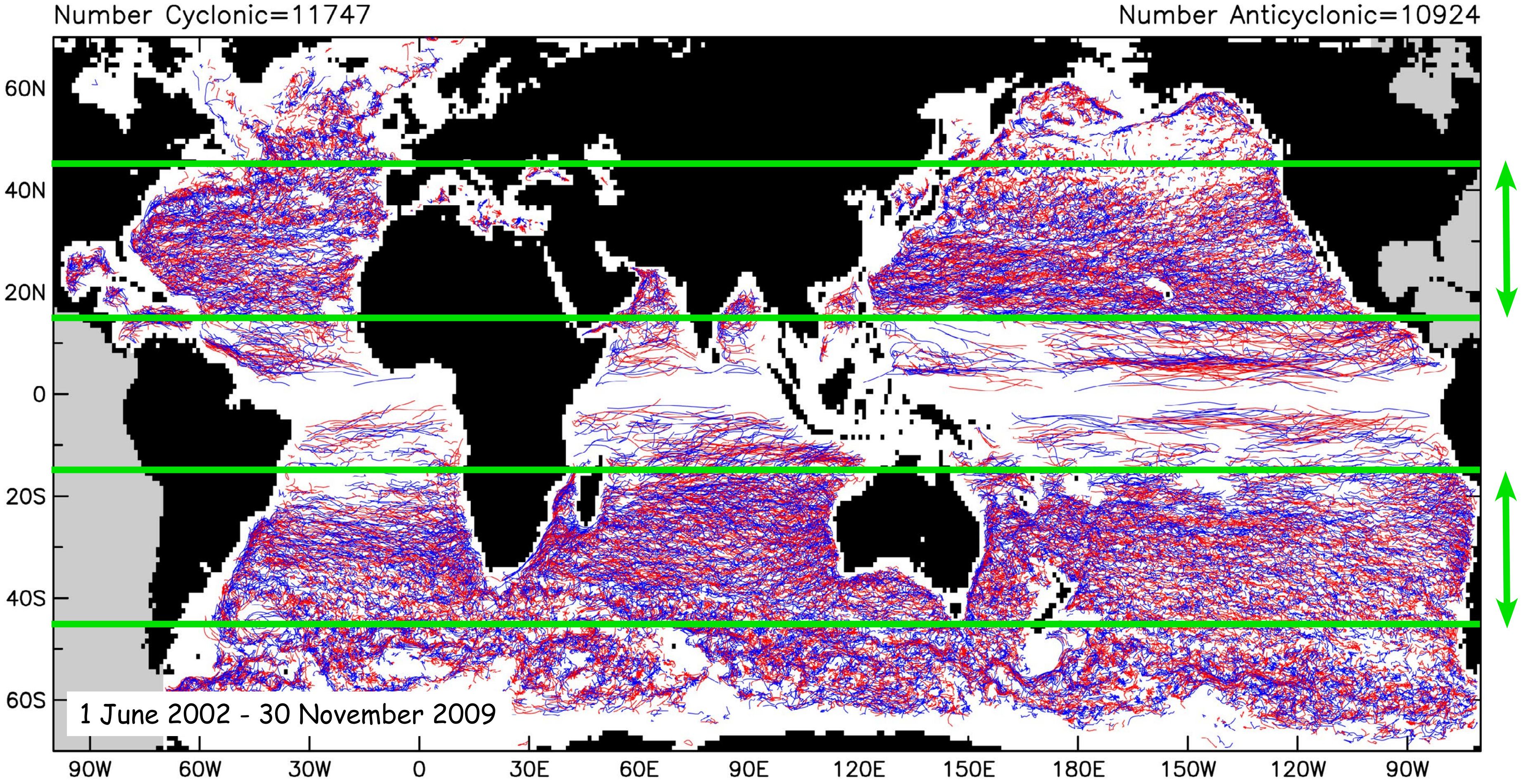

http://cioss.coas.oregonstate.edu/eddies/

Schematic of Eddy Influence on SST Showing the Dependence on Rotational Sense and the Large-Scale SST Gradient

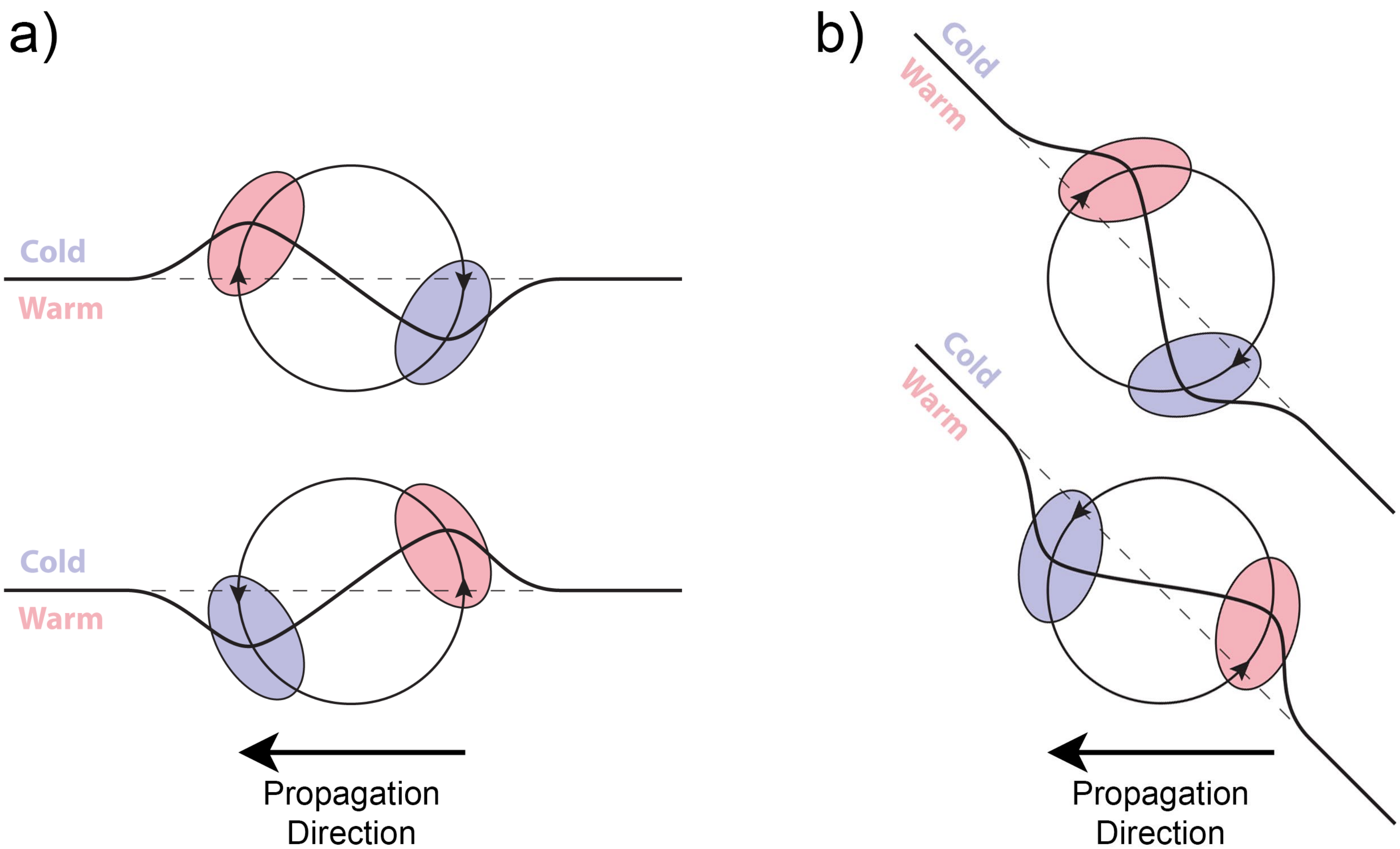

From Gaube et al. (2015)

Global Composite Averages of SST in Eddy-Centric Coordinates

Regions of Southward ∇T

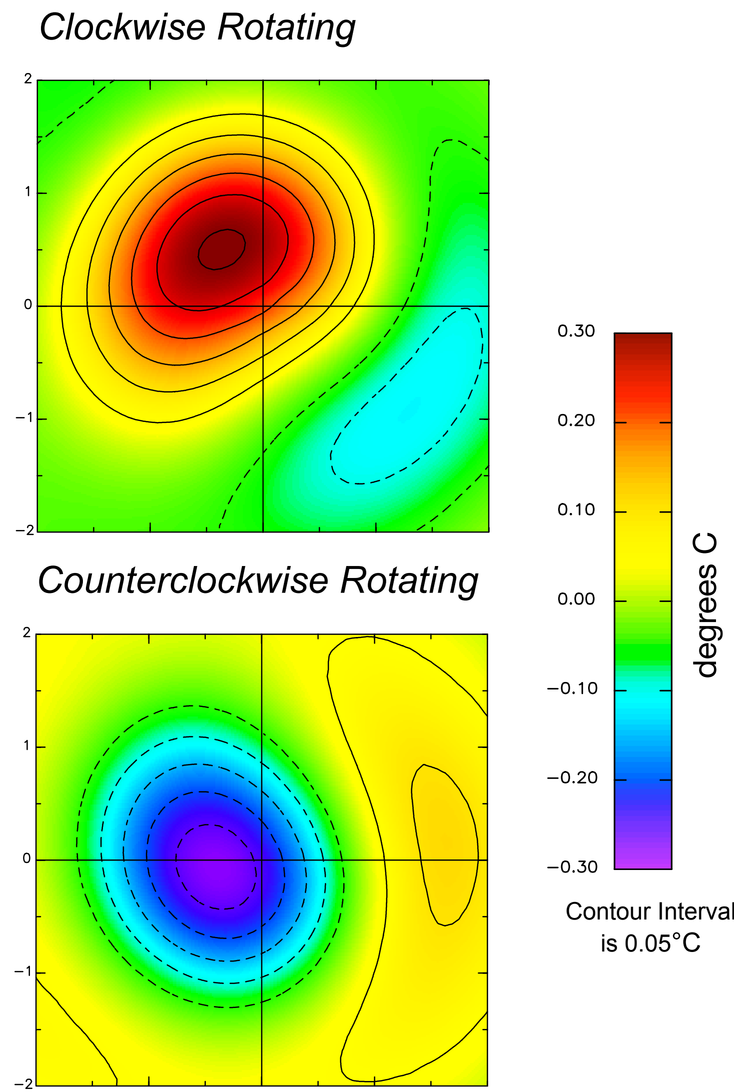

Normalized Distance from Eddy Centroid

Global Composite Averages of SST in Eddy-Centric Coordinates

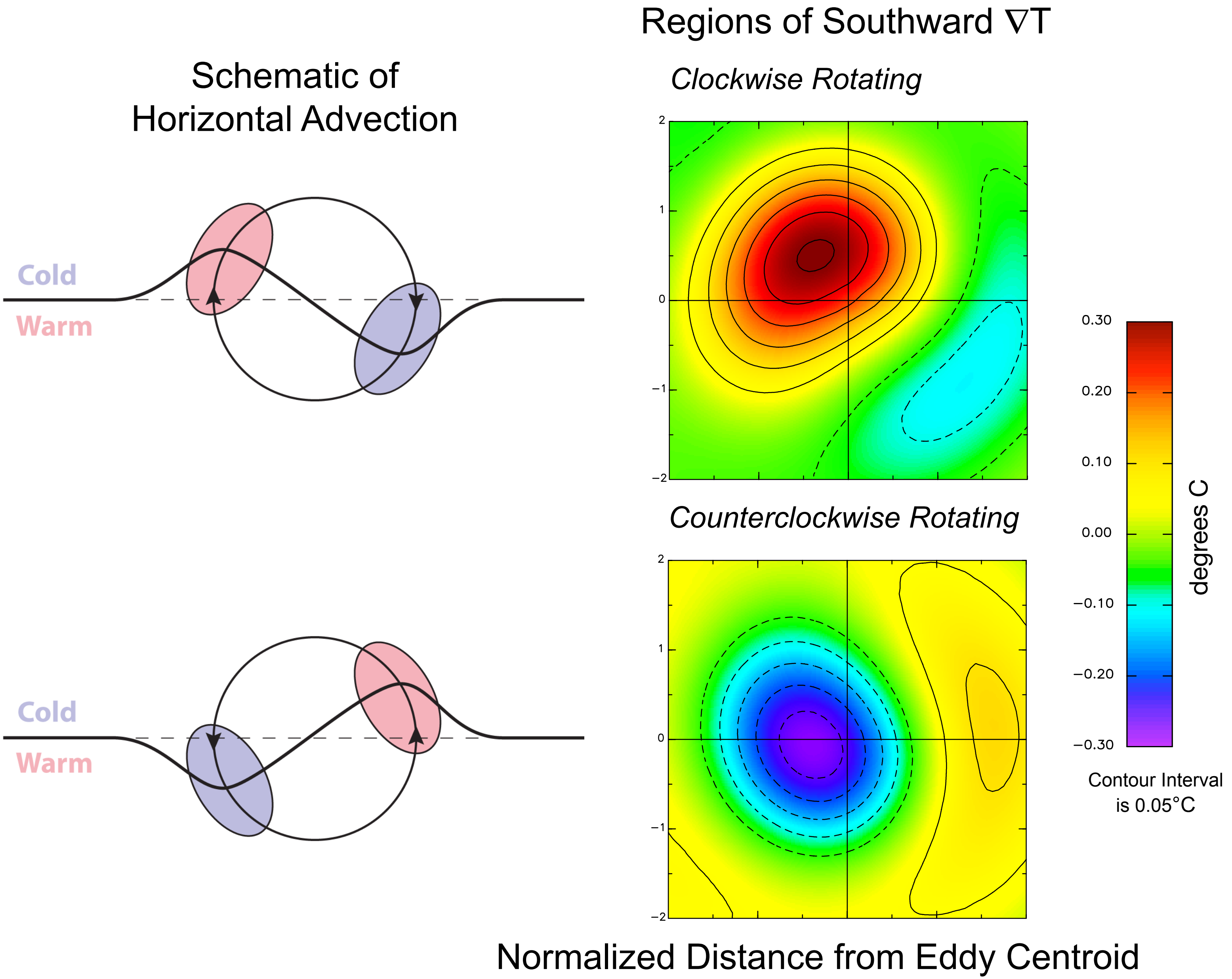

Global Composite Averages of SST in Eddy-Centric Coordinates

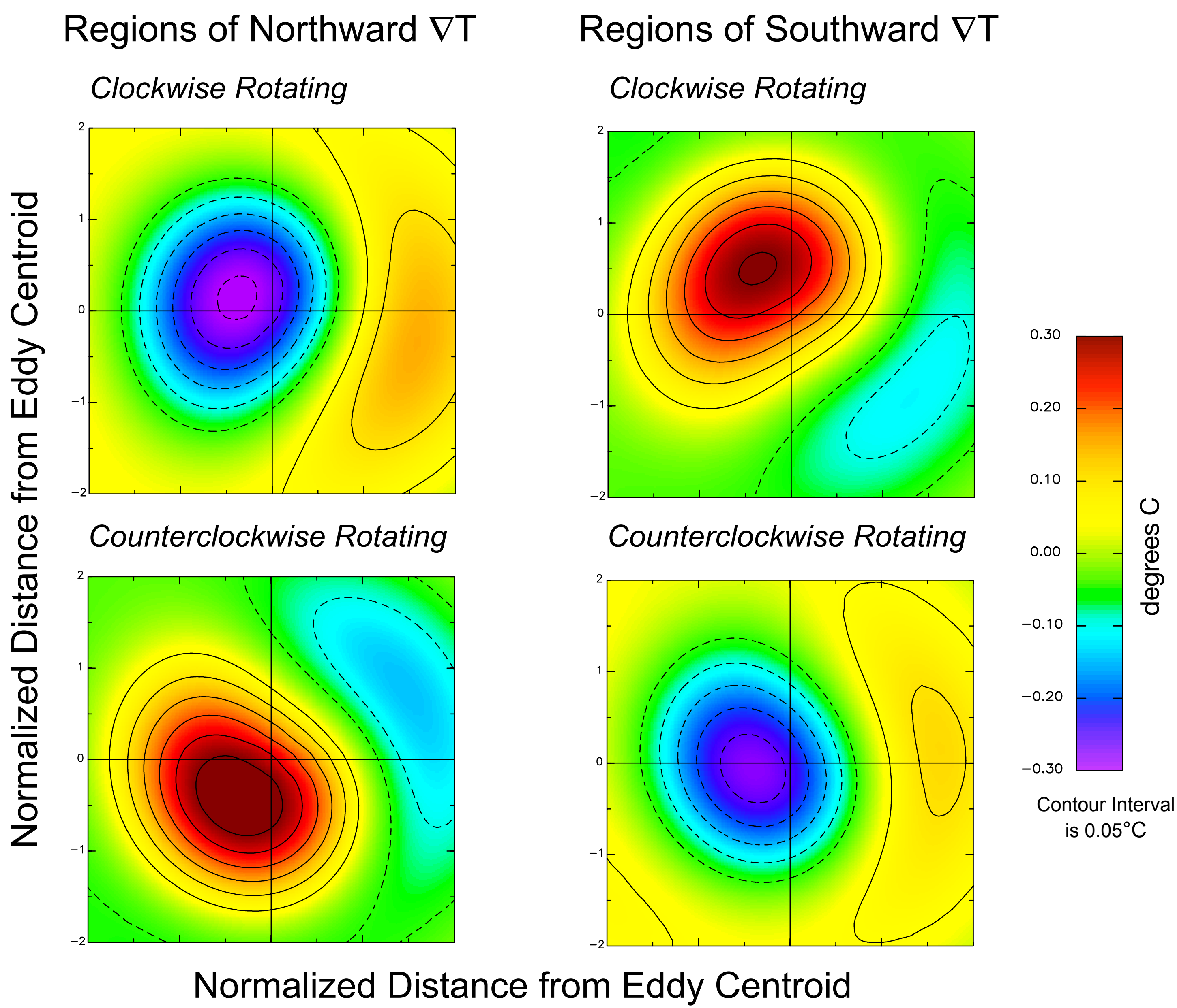

Global Composite Averages of Wind Speed in Eddy-Centric Coordinates

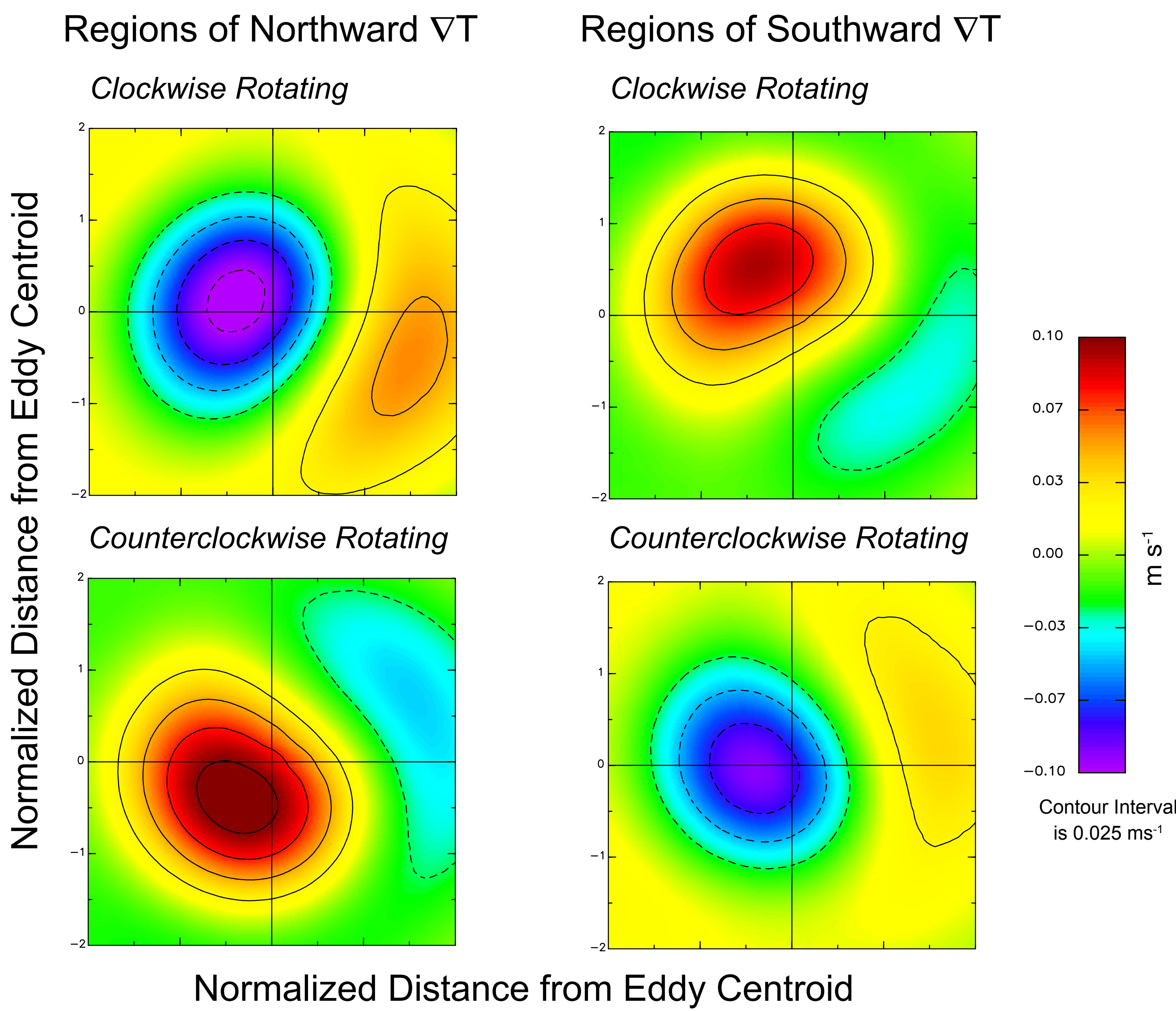

Coupling Coefficient Between Wind Speed and SST over Globally Distributed Mesoscale Eddies

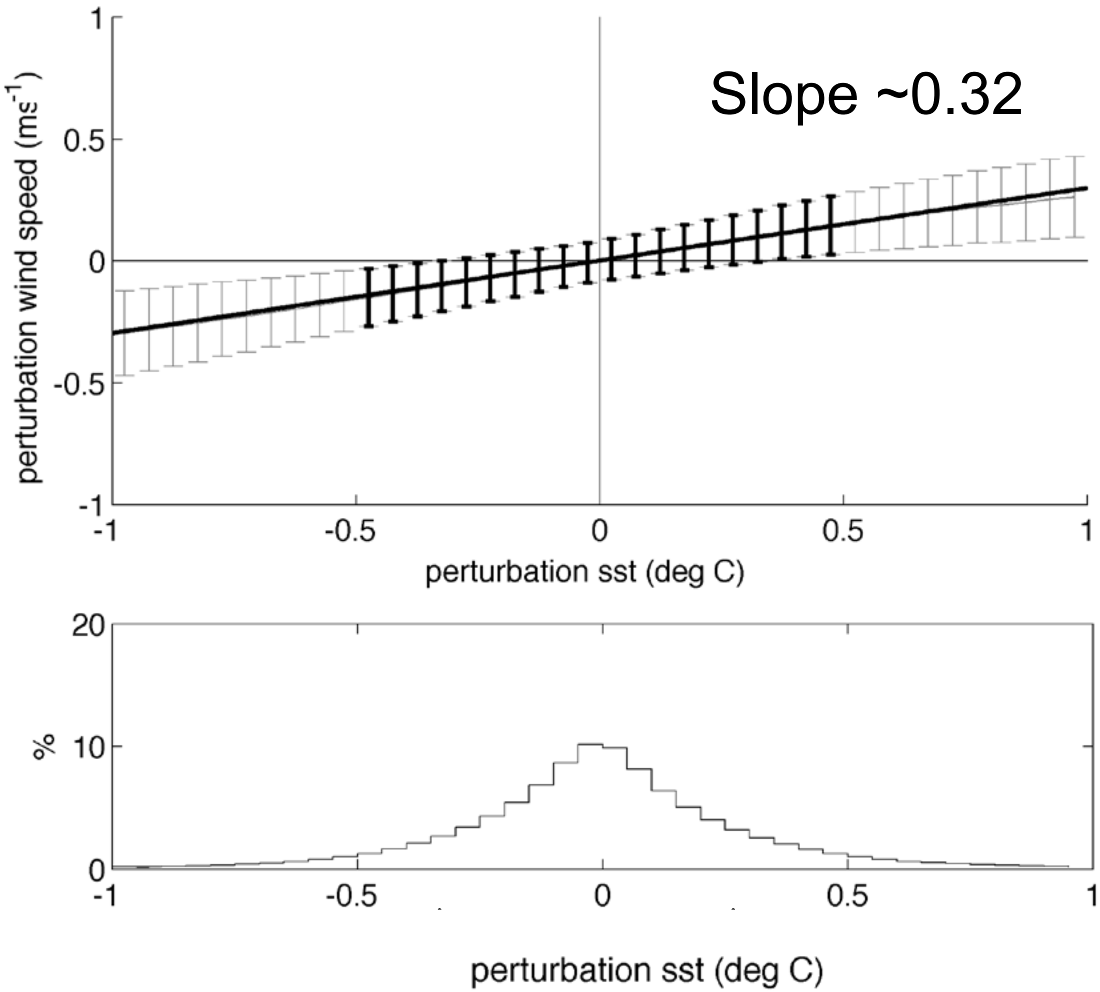

This wind speed response to SST over eddies is consistent with the coupling deduced previously over frontal regions by O'Neill et al. (2010; 2012)

The Coupling Between SST and Wind Speed in 4 Frontal Regions

(Gulf Stream, Kuroshio Extension, Agulhas Return Current and Brazil-Malvinas Current)

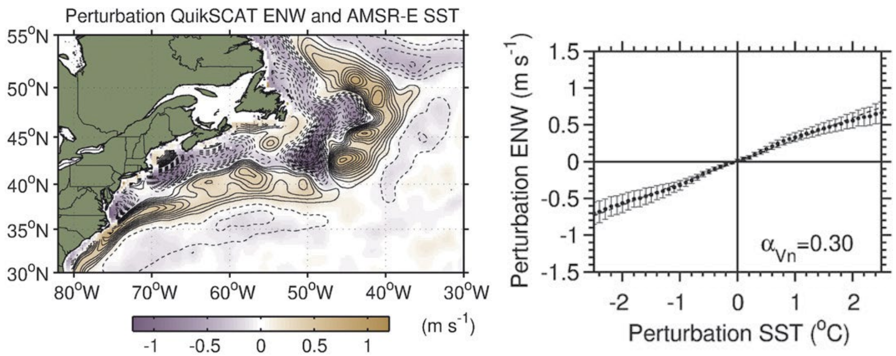

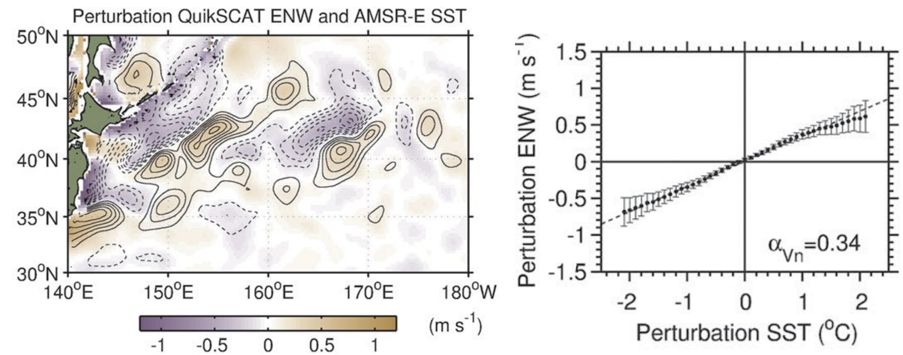

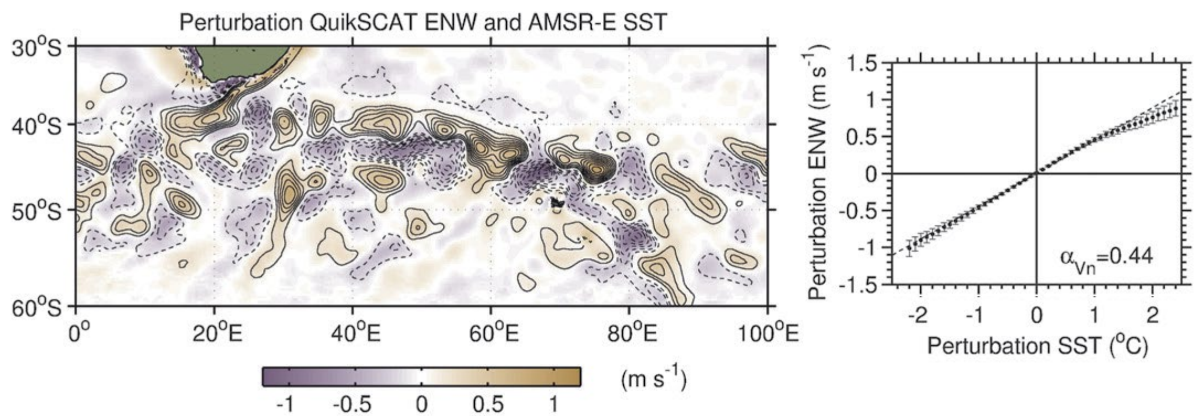

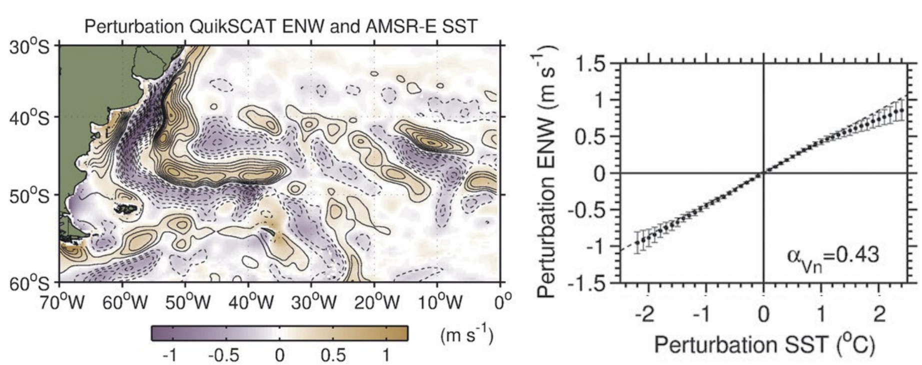

June 2002 - May 2009
Averages

From O'Neill et al. (2012, J. Clim.)

Eddy-induced SST influence on Ekman pumping

Classical Ekman Pumping

In the classical view, the vertical velocity from wind-driven Ekman pumping is

$$w_{Ek} = \frac{1}{\rho_0} \nabla \times \left(\frac{\vec{\tau}}{f} \right) \approx \frac{1}{\rho_0 f} \nabla \times \vec{\tau},$$

where ρ_0 is the water density, f is the planetary vorticity and $\vec{\tau}$ is the wind stress.

The contribution from SST-induced perturbations of the wind stress field is

$$w_{SST} = -\frac{\alpha}{\rho f} \frac{\partial T}{\partial n},$$

where n is the local crosswind spatial coordinate oriented 90° counterclockwise from the large-scale wind direction and α is the coupling coefficient between the wind stress curl and the crosswind SST gradient.

Calculated SST-Induced Ekman Pumping for Westerly Winds over Northern Hemisphere Mesoscale Eddies

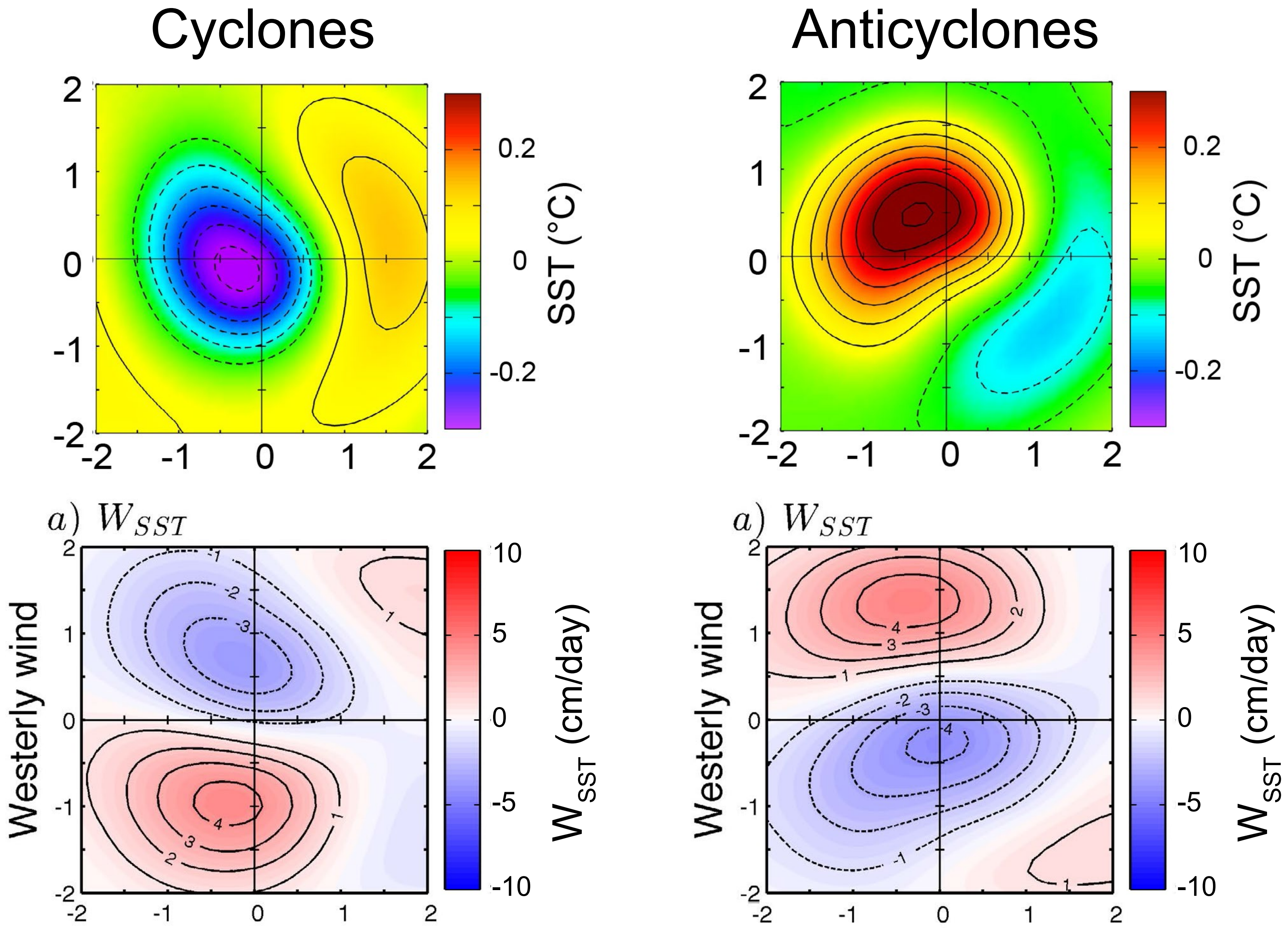

Eddy-induced surface current influence on Ekman pumping

A Complete Analysis of Ekman Pumping (Stern, 1965)

Stern (1965, *Deep-Sea Research*) shows that the planetary vorticity f should be replaced with the *absolute vorticity* $(f + \zeta)$, where $\zeta = \partial v_o / \partial x - \partial u_o / \partial y$ is the relative vorticity.

The "Stern-Ekman pumping" velocity is

$$w_{SE} = \frac{1}{\rho_0} \nabla \times \left(\frac{\vec{\tau}}{f + \zeta} \right) \approx \underbrace{\frac{1}{\rho_0 f} \nabla \times \vec{\tau}}_{w_{SST} + w_c} + \underbrace{\frac{1}{\rho_0 f^2} \left(\tau_x \frac{\partial \zeta}{\partial y} - \tau_y \frac{\partial \zeta}{\partial x} \right)}_{w_\zeta}$$

where

$$w_{SST} = -\frac{\alpha}{\rho f} \frac{\partial T}{\partial n}$$

$$w_c = \frac{\rho_a C_D}{\rho_0 f} \nabla \times \left[(\vec{u}_a - \vec{u}_o) \left| \vec{u}_a - \vec{u}_o \right| \right]$$ ($\vec{u}_a - \vec{u}_o$ is the relative wind)

$$w_\zeta = \frac{1}{\rho_0 f^2} \left(\tau_x \frac{\partial \zeta}{\partial y} - \tau_y \frac{\partial \zeta}{\partial x} \right)$$

Ekman Pumping for an Idealized Cyclone

(from Gaube et al., 2015, *J. Phys. Oceanogr.*)

SST-Induced Ekman Pumping

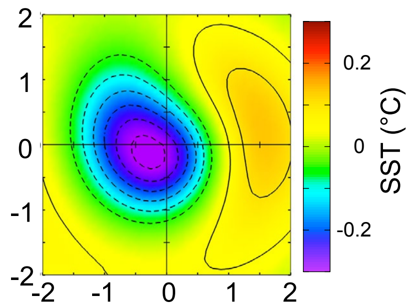

Current-Induced Ekman Pumping

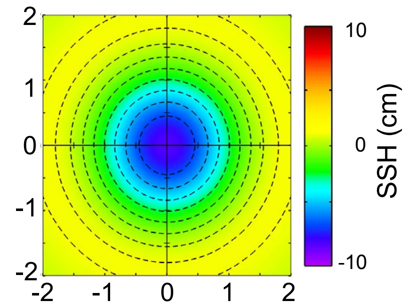

Ekman Pumping for an Idealized Cyclone

(from Gaube et al., 2015, *J. Phys. Oceanogr.*)

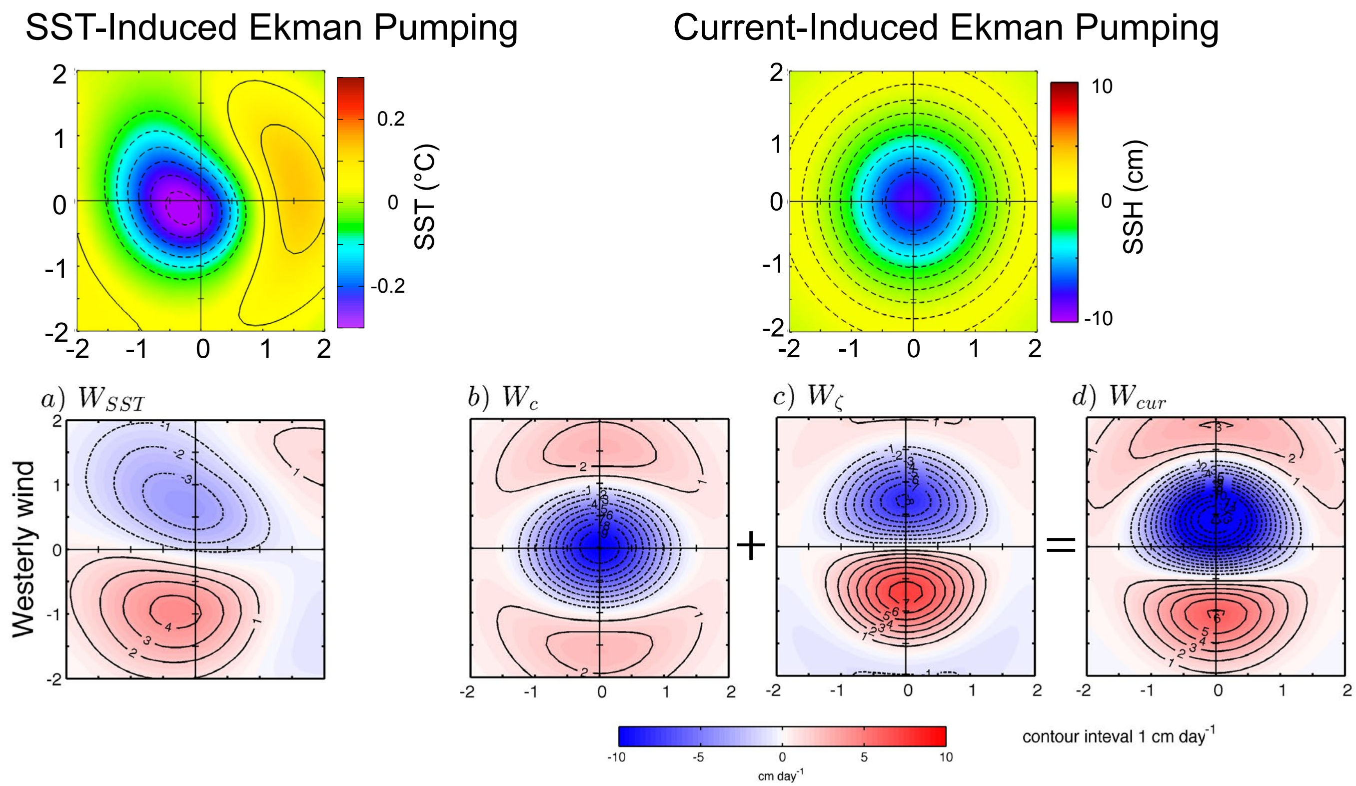

Ekman Pumping for an Idealized Cyclone

(from Gaube et al., 2015, *J. Phys. Oceanogr.*)

SST-Induced Ekman Pumping

Current-Induced Ekman Pumping

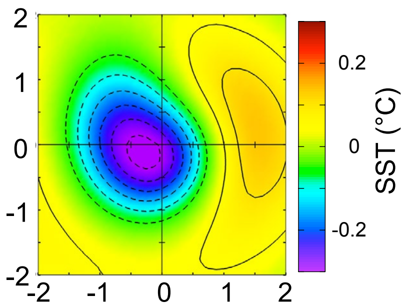

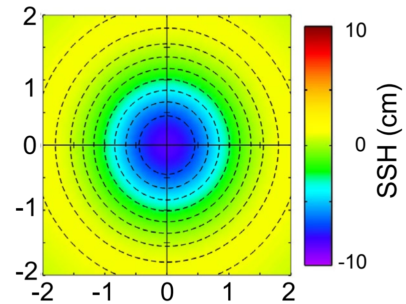

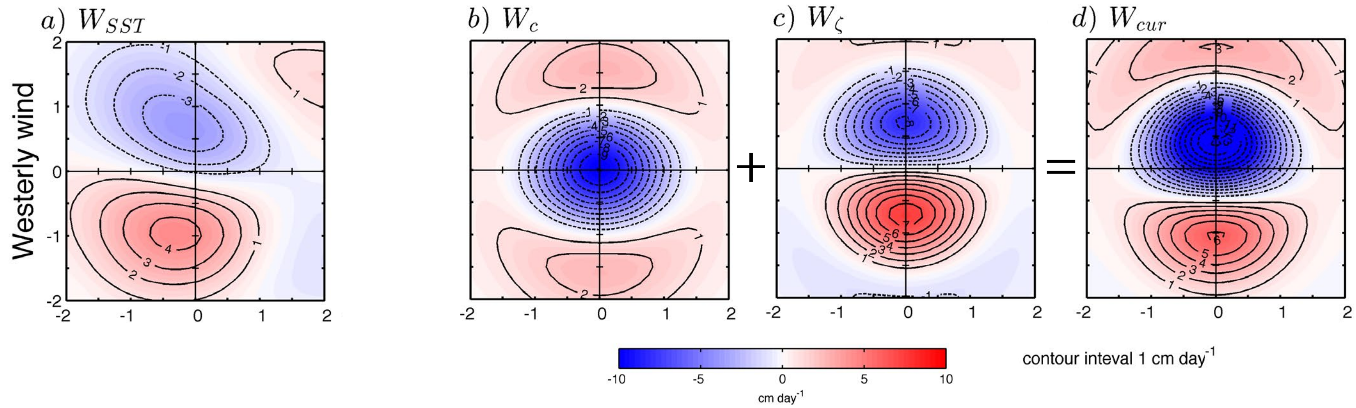

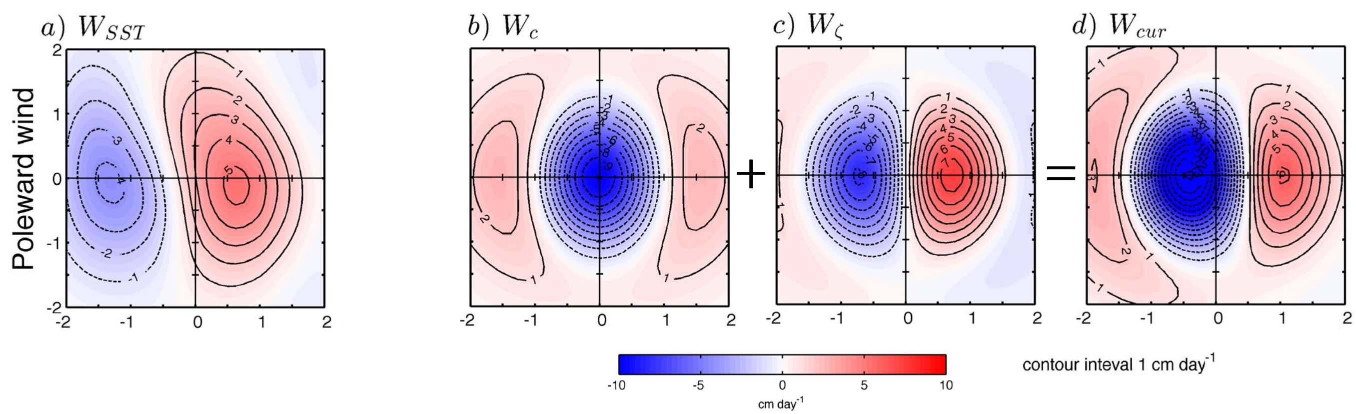

Ekman Pumping for an Idealized Anticyclone

(from Gaube et al., 2015, *J. Phys. Oceanogr.*)

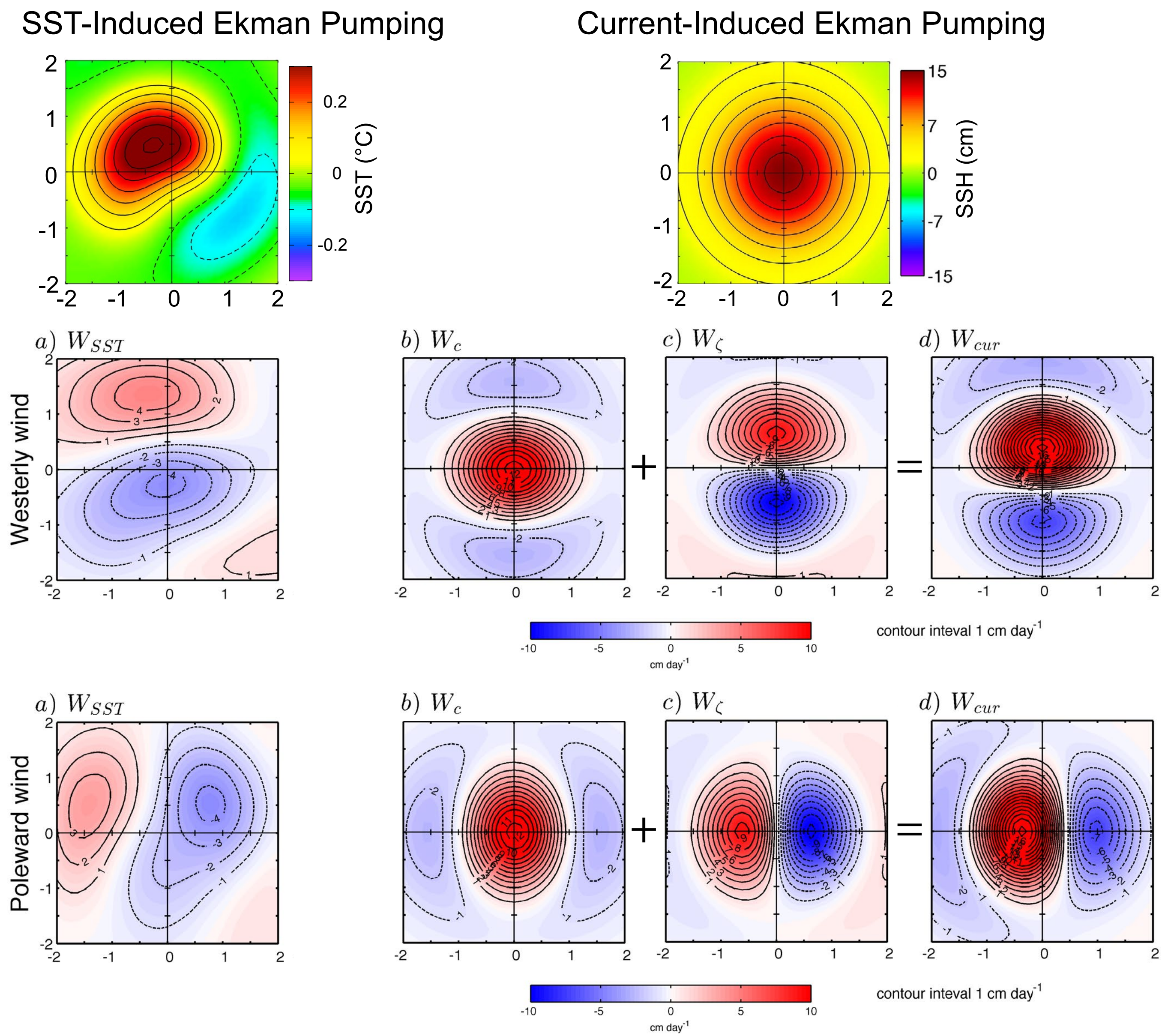

Validation of Total Ekman Pumping

Calculated for N. Hemisphere Eddies from SST, SSH and Large-Scale Winds

(from Gaube et al., 2015, J. Phys. Oceanogr.)

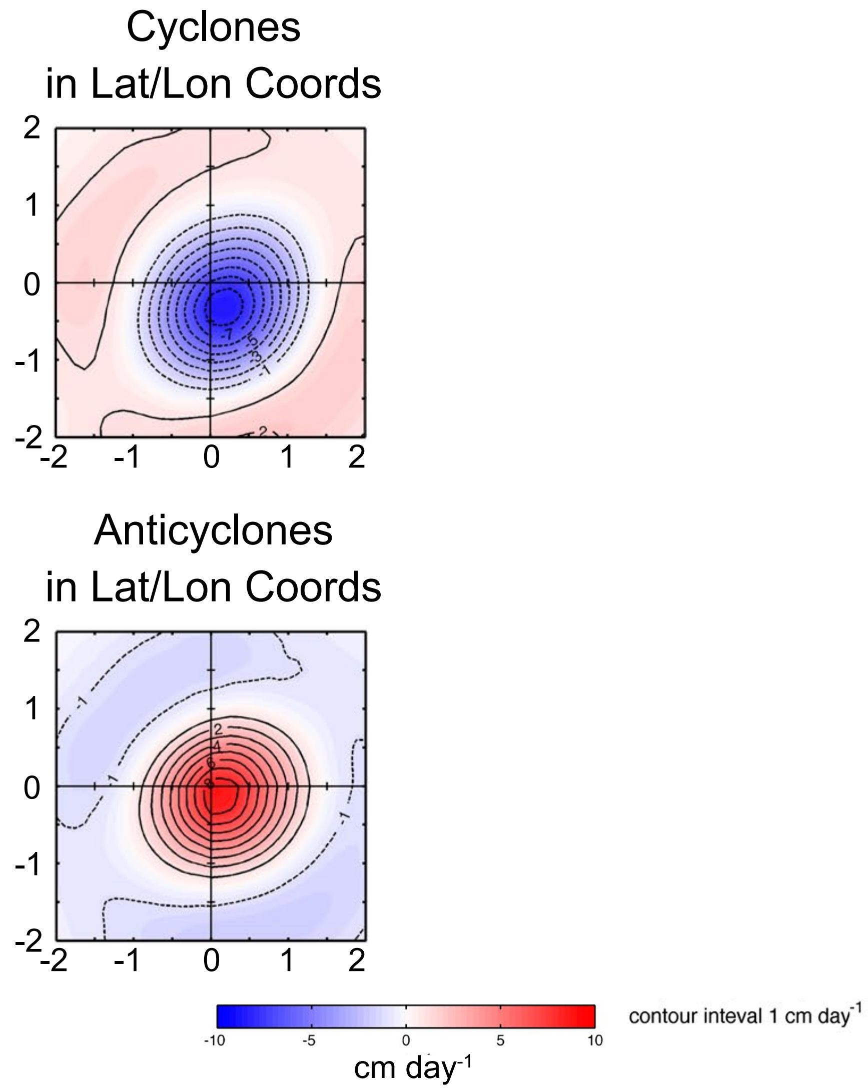

Validation of Total Ekman Pumping

Calculated for N. Hemisphere Eddies from SST, SSH and Large-Scale Winds

(from Gaube et al., 2015, J. Phys. Oceanogr.)

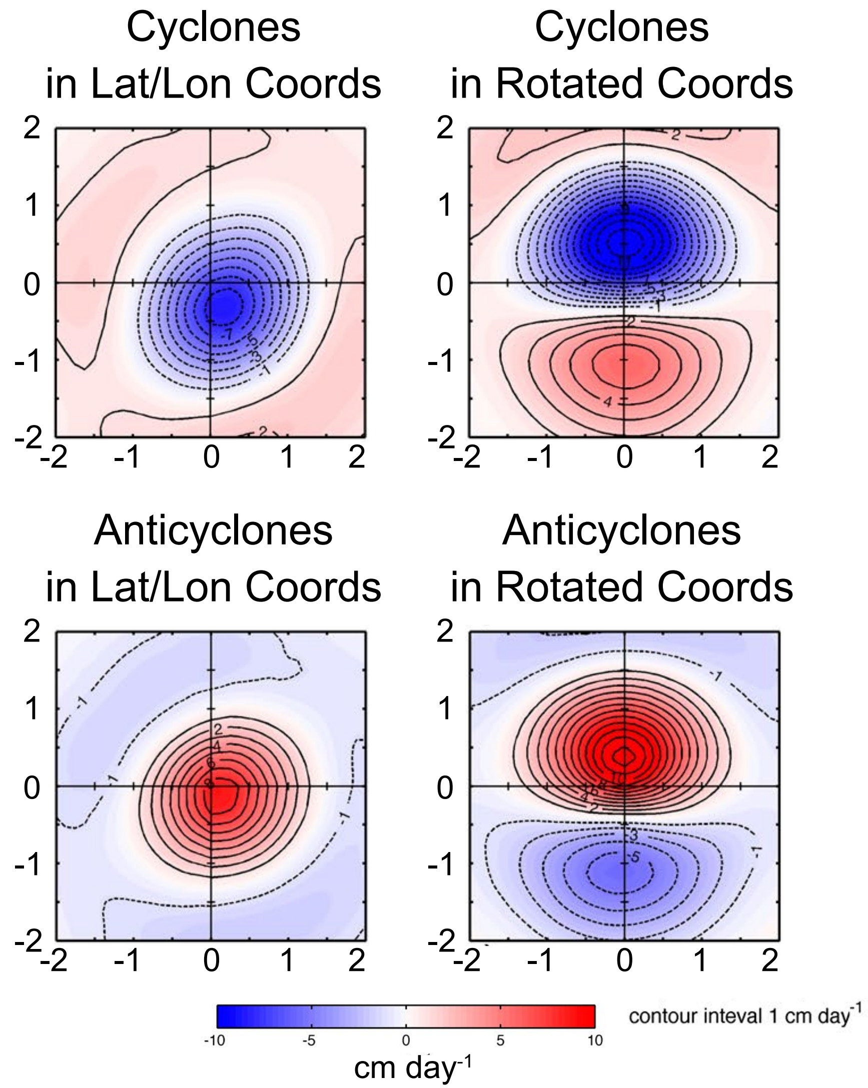

Validation of Total Ekman Pumping

Calculated for N. Hemisphere Eddies from SST, SSH and Large-Scale Winds

(from Gaube et al., 2015, J. Phys. Oceanogr.)

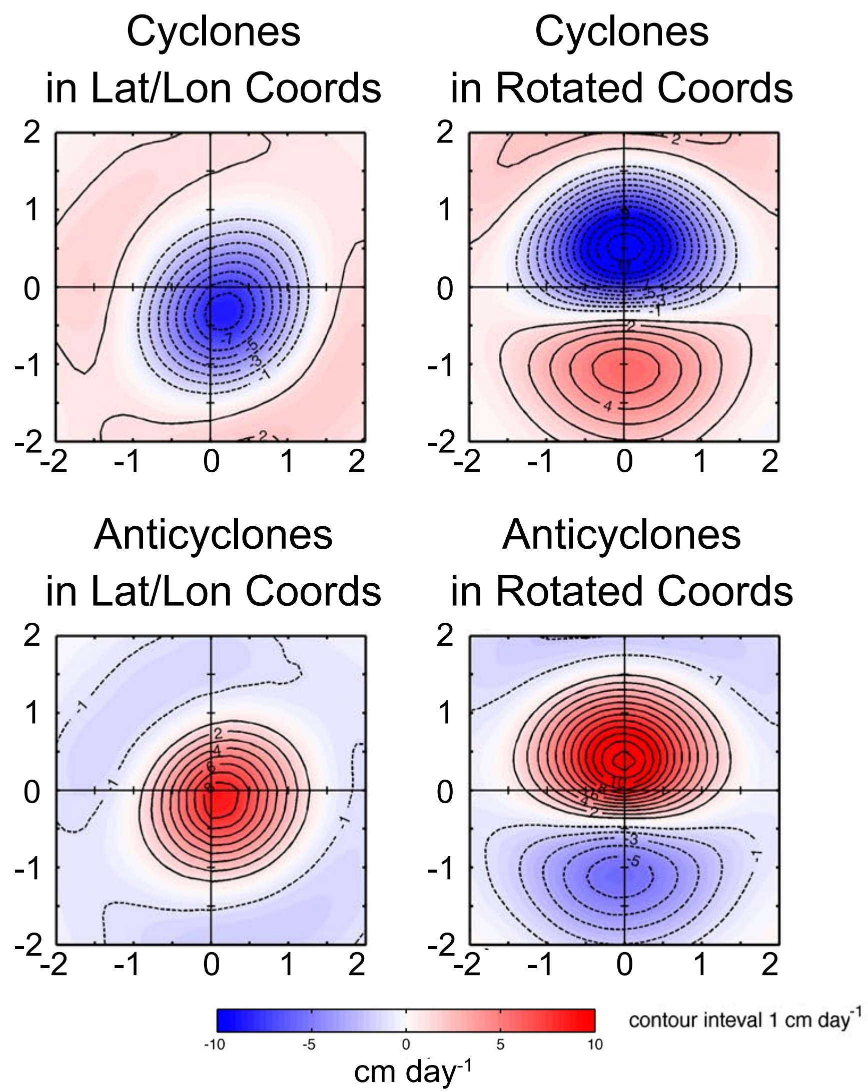

In the composite averages in latitude/longitude coordinates, note that:

- downwelling occurs in anticyclones
- upwelling occurs in cyclones

Large-Scale Context: Climatological Average Ekman pumping

(From Risien and Chelton, 2008, J. Phys. Oceanogr.)

January July

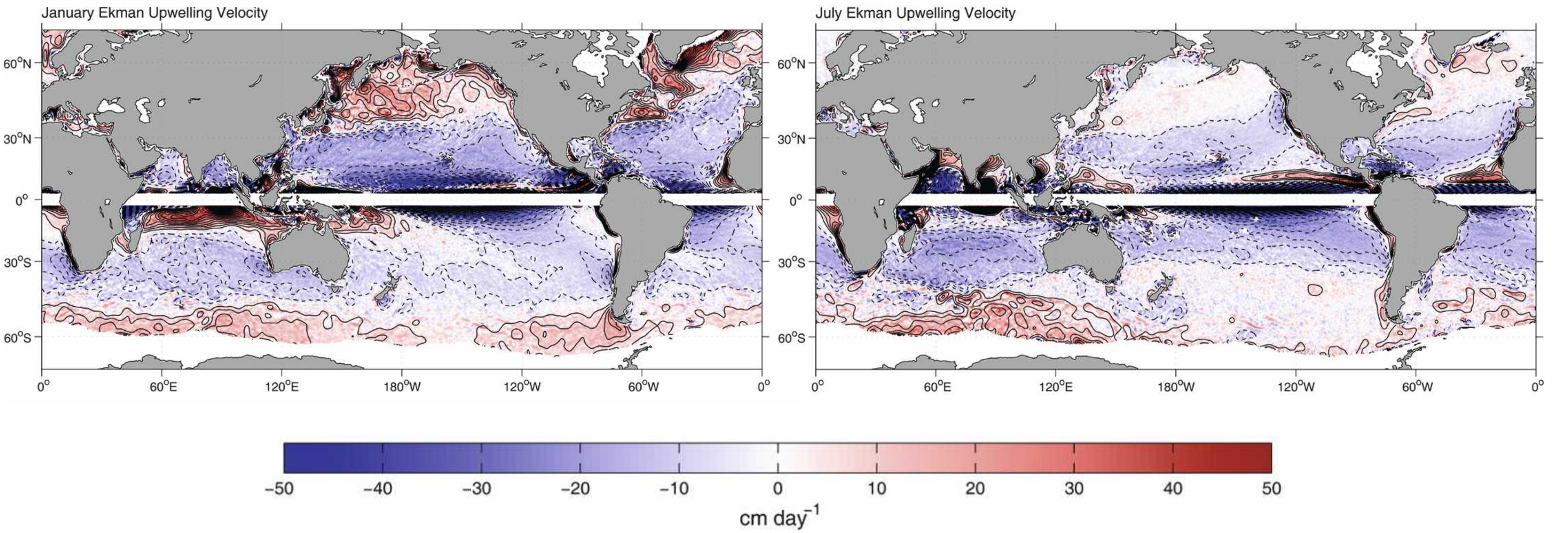

A typical Ekman upwelling velocity on these large scales is ~20 cm/day

Eddy Kinetic Energy at 10 m from ROMS Simulations With and Without SST and Current Feedbacks

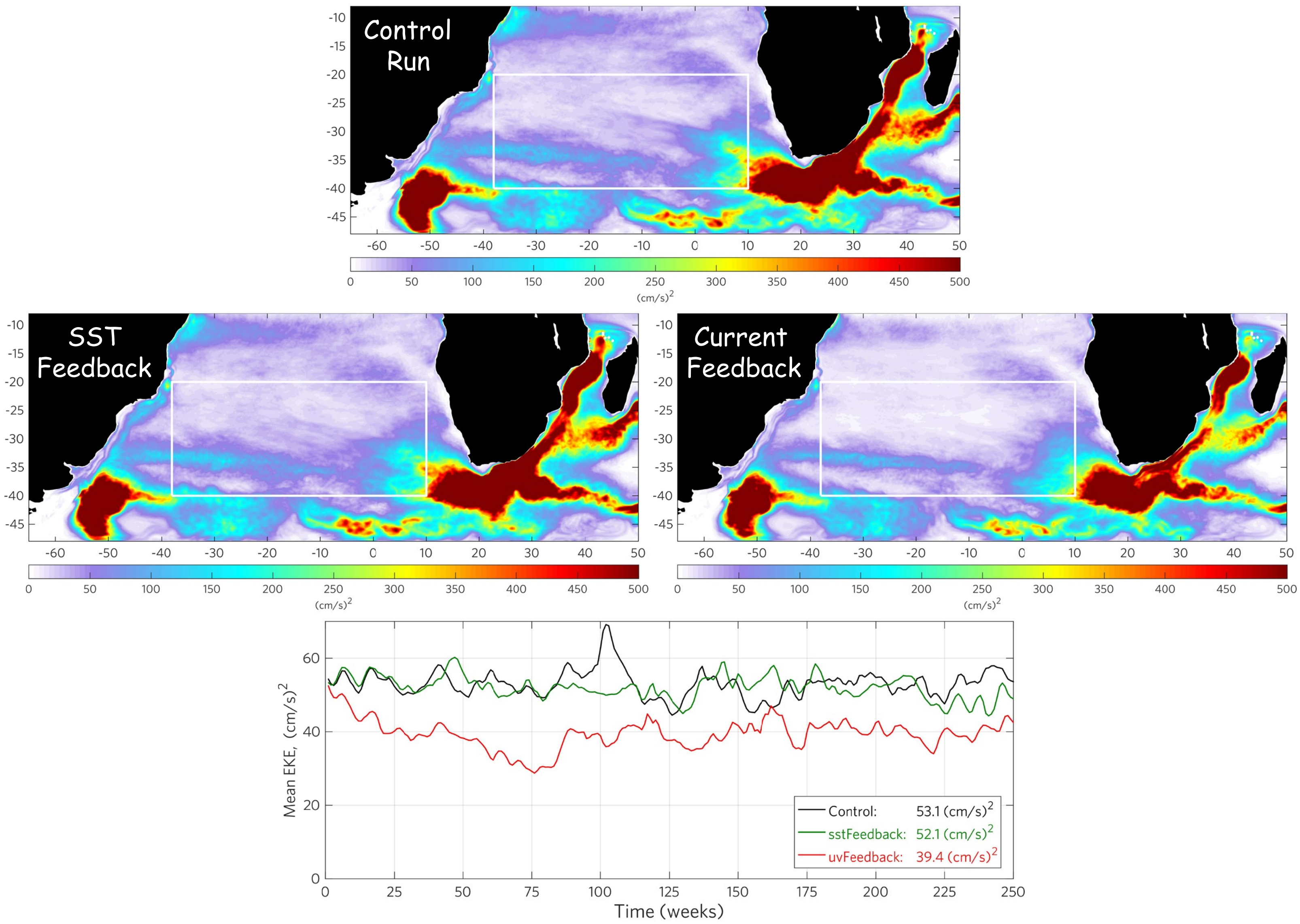

Composite Averages of Vertical Profiles of Maximum Pressure Anomalies

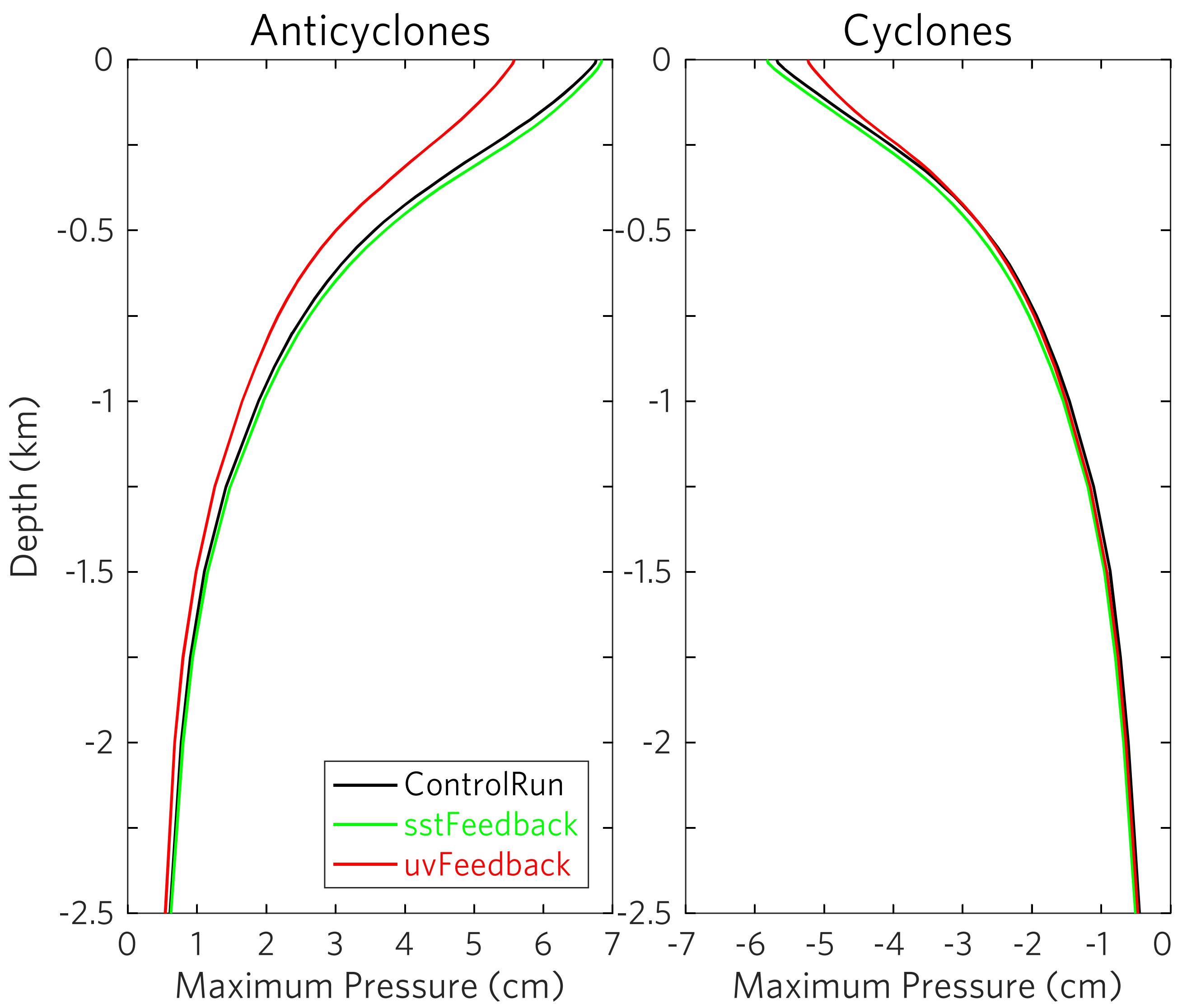

Extra Figures

Schematic Summary of SST Influence on the Wind Speed Profile in the Marine Atmospheric Boundary Layer

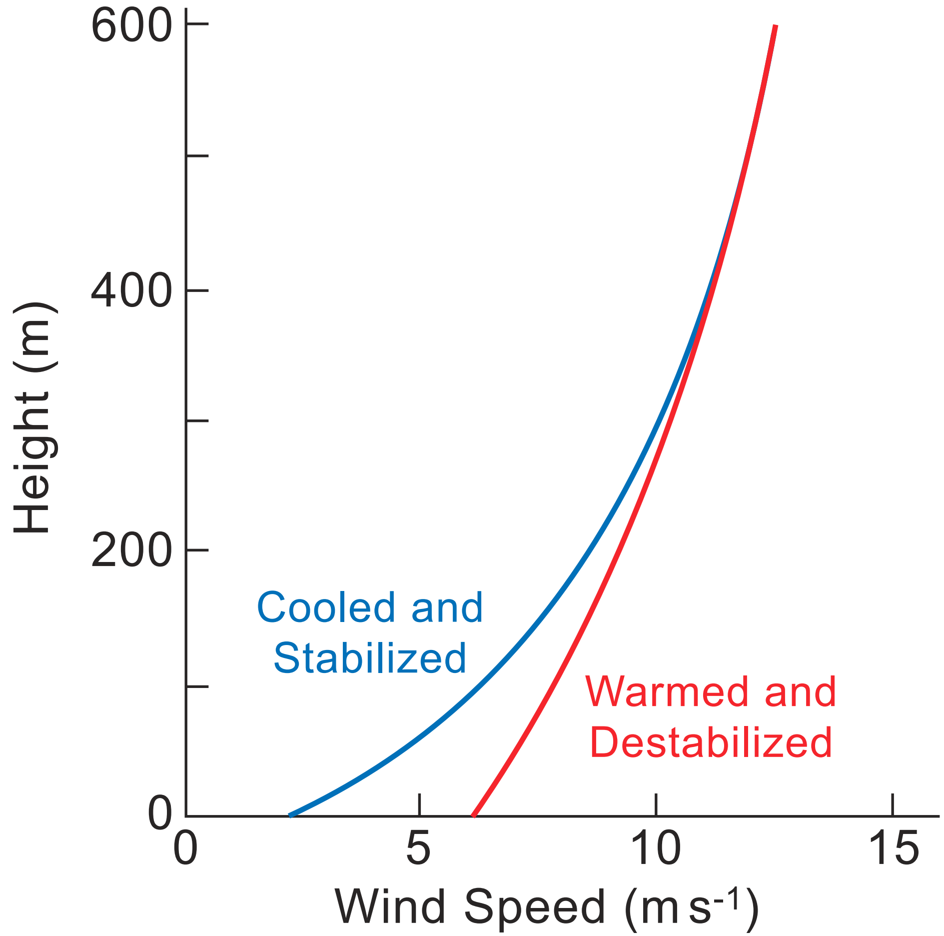

This is similar to diurnal variation of the atmospheric boundary layer over land:

- *nocturnal stable boundary layer from radiative cooling*
- *daytime unstable boundary layer from solar heating of the land*

Note that vertical turbulent mixing is not the only term that is important in the momentum balance. The nonlinear advection and pressure gradient terms are also important, especially the latter.

This coupling between SST and winds on scales smaller than ~1000 km is opposite the negative correlation that occurs on basin scales:

- surface winds are <u>positively</u> correlated with SST on oceanic mesoscales.

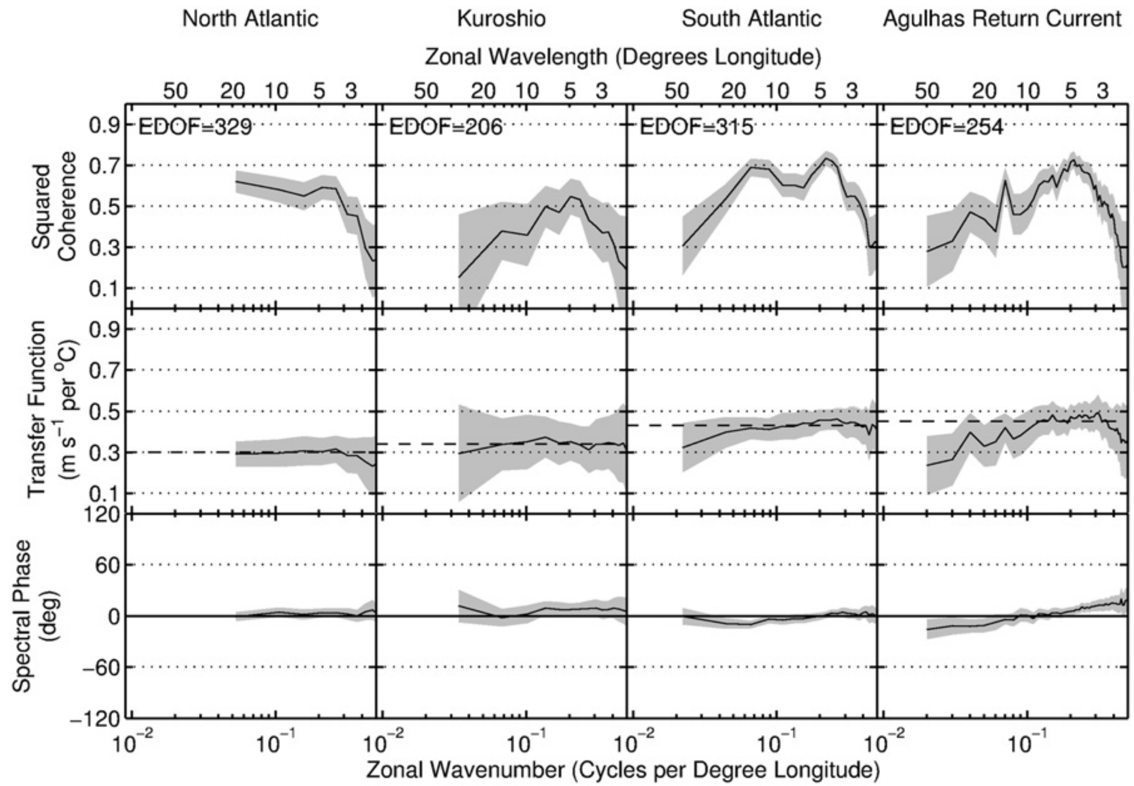

FIG. 3. Cross-spectral statistics of the QuikSCAT ENW and AMSR-E SST as functions of zonal wavenumber: (top) squared coherence, (middle) transfer function, and (bottom) spectral phase. The four regions of interest here are noted above each column of panels. These statistics were computed from monthly averaged QuikSCAT ENW and AMSR-E SST fields over the period June 2002–May 2009. Only cross-spectral statistics where the squared coherences are statistically significant above the 95% confidence level are shown, and 95% confidence intervals of the statistics are shown by the gray shading in each panel (estimated according to p. 317 in Bendat and Piersol 1986). Estimates of the equivalent degrees of freedom (EDOF) of the cross-spectral estimates are shown in each column of panels. The corresponding zonal wavelengths in degrees longitude are shown at the top of the figure. The dashed horizontal lines in the middle row of panels are the slopes of the regression lines for the binned scatterplots in Figs. 4–7 for the spatially high-pass-filtered ENW and SST.

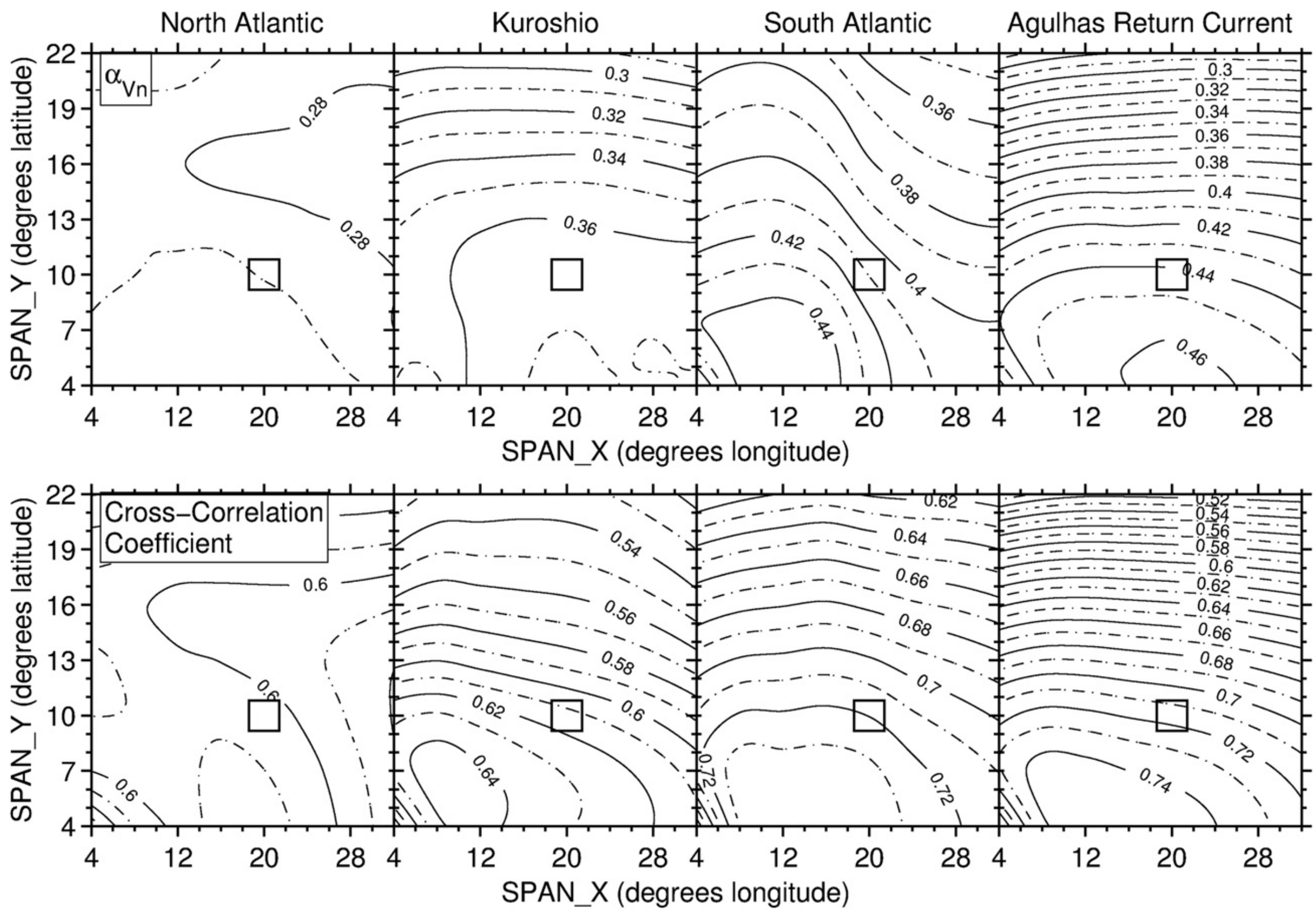

FIG. 8. (top) The coupling coefficient α_{vn} and (bottom) cross-correlation coefficient between the ENW and SST perturbations computed from the monthly-averaged QuikSCAT ENW and AMSR-E SST as a function of the zonal and meridional half-spans of the loess spatial high-pass filter (denoted as SPAN_X and SPAN_Y, respectively; the loess filter was discussed briefly in section 2b). The y axis represents the meridional half-span and the x axis represents the zonal half-span. Because of the computational expense of computing the spatially high-pass-filtered fields, the coupling coefficients were computed only for the 2-yr period June 2002–May 2004 at monthly intervals. The α_{vn} estimates and cross-correlation coefficients were computed from spatially high-pass-filtered ENW and SST fields using an interval of 4° longitude for SPAN_X and 3° latitude for SPAN_Y. The contour interval is 0.01 $\mathrm{m\ s^{-1}\ {}^{\circ}C^{-1}}$ in the top row and 0.01 in the bottom row, and every other contour is dashed–dotted to improve clarity. The SPAN_X of 20° longitude and SPAN_Y of 10° latitude used in this analysis are shown in each panel by the square.